Correlations for Vapor Nucleating Critical Embryo Parameters[a)]

Lars-Erik Magnusson[b)] and John A. Koropchak[c)]
Department of Chemistry and Biochemistry, Southern Illinois University, Carbondale, Illinois 62901-4409

Michael P. Anisimov and Valeriy M. Poznjakovskiy
Department of Chemical Engineering, Clarkson University, Potsdam, New York 13699-5707 and Aerosol Nucleation Lab at Kemerovo, IC SB RAS, 41A-119 Moskovskiy Prospect, 650065 Kemerovo, Russia

Juan Fernandez de la Mora
Mechanical Engineering Department, Yale University, 9 Hillhouse Avenue, New Haven, Connecticut 06520-8286

(Received 30 May 2002; revised 21 December 2002; accepted 30 December 2002; published 18 July 2003)

Condensation nucleation light scattering detection in principle works by converting the effluent of the chromatographic separation into an aerosol and then selectively evaporating the mobile phase, leaving less volatile analytes and nonvolatile impurities as dry aerosol particles. The dry particles produced are then exposed to an environment that is saturated with the vapors of an organic solvent (commonly *n*-butanol). The blend of aerosol particles and organic vapor is then cooled so that conditions of vapor supersaturation are achieved. In principle, the vapor then condenses onto the dry particles, growing each particle (ideally) from as small as a few nanometers in diameter into a droplet with a diameter up to about 10 μm. The grown droplets are then passed through a beam of light, and the light scattered by the droplets is detected and used as the detector response. This growth and detection step is generally carried out using commercial continuous-flow condensation nucleus counters. In the present research, the possibility of using other fluids than the commonly used *n*-butanol is investigated. The Kelvin equation and the Nucleation theorem [Anisimov *et al.* (1978)] are used to evaluate a range of fluids for efficacy of growing small particles by condensation nucleation. Using the available experimental data on vapor nucleation, the correlations of Kelvin diameters (the critical embryo sizes) and the bulk surface tension with dielectric constants of working liquids are found. A simple method for choosing the most efficient fluid, within a class of fluids, for growth of small particles is suggested. © 2003 American Institute of Physics. [DOI: 10.1063/1.1555590]

Contents

List of Tables

[a)]Dedicated to Professor James Neckers on the occasion of his 100th Birthday.
[b)]Present address: Pfizer Global Research and Development, Ann Arbor, MI.
[c)]Electronic mail: koropcha@siu.edu

List of Figures

1. Introduction

1.1. Background

Condensation nucleation light scattering detection (CNLSD) is a relatively new aerosol-based analytical separations detection technique, which was first introduced as a detector for high-performance liquid chromatography (HPLC) by Allen and Koropchak (1993). Among the goals of the CNLSD project is the development of sensitive and universal detection for various analytical separation methods, such as HPLC and capillary electrophoresis (CE).

CNLSD in principle works by converting the effluent of the chromatographic separation into an aerosol—generally using pneumatic nebulization for liquid chromatographic and electrospray (ES) for capillary electrophoretic separations [see Szostek *et al.* (1997)]—and then selectively evaporating the mobile phase, leaving less volatile analytes and nonvolatile impurities as dry aerosol particles. The dry particles produced are then exposed to an environment that is saturated with the vapors of an organic solvent (commonly *n*-butanol). The blend of aerosol particles and organic vapor is then cooled so that conditions of vapor supersaturation are achieved. In principle, the vapor then condenses onto the dry particles (condensation nucleation), growing each particle (ideally) from as small as a few nanometers in diameter into a droplet with a diameter up to about 12 μm [Agarwal and Sem (1980)]. The grown droplets are then passed through a beam of light, and the light they scatter is detected and used as the detector response. This growth and detection step is generally carried out using commercial continuous-flow condensation nucleus counters (CNCs) [e.g., see McMurry (2000)]—often referred to as condensation particle counters (CPCs)—although much of the early work was done with a home-built detector [e.g., Allen and Koropchak (1993)]. The CNC most commonly used for CNLSD is the UCPC 3025A (TSI, St Paul, Minnesota).

This growth of nanometer-sized particles into 12 μm droplets is a process with very large gains in mass ($\sim 10^{11}$) and light-scattering efficiency (compared to detecting the dry particles directly without growth). In analytical chemistry terms, the limit of detection (LOD) achieved has been as low as 10 $\mu g\cdot L^{-1}$ in some cases and calibration curves have been found to be generally linear. Two reviews of CNLSD have been published [Koropchak *et al.* (1999); Koropchak, *et al.* (2000)].

As a first approximation, the response of CNLSD for capillary separations depends on the overlap between the detection efficiency curve (DEC) of the CNC and the particle-size distribution (PSD) of the dry aerosol particles. The size of these dry particles is related to the initial wet droplet diameter (d_{wet}), nonvolatile concentration (C), and density (ρ) by an equation derived from simple volume–density relationships [see also Chen *et al.* (1995)]:

$$d_{dry} = d_{wet}\left(\frac{C}{\rho}\right)^{1/3}.$$

Since the size of the particles increases with increasing analyte concentration, and since the detection efficiency increases for larger particles [e.g., Kesten *et al.* (1991)], the response becomes greater for higher concentrations. Thus, the smallest analyte concentration that can be detected (LOD) is limited by the lower-size threshold for particle growth in the CNC (assuming that nonvolatile contaminants in the background are not a limiting factor). Thus, if the size threshold could be lowered, smaller particles could be detected and the sensitivity of the detector would be improved.

The advantage of lowering the size threshold for particle detection from about 3 to about 2 nm or less is illustrated schematically in Fig. 1. This figure shows the overlap of two detection efficiency curves, DEC-A, having a size threshold of less than about 2 nm and DEC-B having a size threshold of about 3 nm, with two particle size distributions: PSD A for a lower analyte concentration and PSD B for a higher analyte concentration. DEC-A represents the curve when using a fluid with a lower Kelvin diameter (e.g., glycerol), while DEC-B represents the curve when using *n*-butanol as the condensing fluid. A CNC with DEC-A would grow and detect most of the particles in PSD A and virtually all of the particles in PSD B, while a CNC with DEC-B (e.g., TSI UCPC 3025A) would grow only PSD B using *n*-butanol vapor.

Another illustration is given in Fig. 2, which gives a cartoon depiction of particles of different sizes that could be grown if different condensing fluids were used. For CNLSD, a lowering of the detection limit (LOD) by almost 1 order of magnitude can be predicted based on a lowered size threshold for particle detection from 3 to 1.5 nm, provided that nonvolatile background material is not a limiting factor.

In the present research, the possibility of using other fluids than the commonly used *n*-butanol is investigated. The Kelvin equation and the Nucleation theorem [Anisimov *et al.* (1978)] are used to evaluate a range of fluids for efficacy of growing small particles by condensation nucleation. A simple method for choosing the most efficient fluid, within a class of fluids, for growth of small particles is devised.

1.2. Prior Work and Present Need

The key step in a condensation nucleation process is the increase in apparent size of a small particle by condensation of a vapor onto the particle. Continuous flow CNCs have up to this date sometimes employed ethanol, but most often *n*-butanol, as the condensing fluid [e.g., McMurry (2000)]. The most popular commercial CNCs, the TSI 3000-series, introduced with the TSI 3020 [Agarwal and Sem (1980)], all use *n*-butanol. This fluid was apparently chosen because it absorbs less water than the initially investigated isopropanol, and because its vapor pressure at near ambient temperatures is suitable for growing droplets large enough for optical detection. Butanol vapor diffusivity in air is also low enough so as to provide a low rate of vapor depletion to the condenser wall [McMurry (2000)]. Recently, water has also been used as the condensing fluid in a continuous flow modified mixing-type CNC [Parsons and Mavliev (2001)]. This instrument was characterized by a lower size threshold for particle detection of about 12 nm. However, because of hardware constraints, the instrument was not optimized for small particle detection, but rather for prolonging the life of the thermoelectric cooler modules used in the condenser. The authors pointed out that one difficulty associated with the use of water is the prevention of rampant microbial growth in the system.

Water has previously been studied as the condensing fluid in various systems. Besides C. T. R. Wilson's early work [see Wilson (1927)], examples include studies of the size-analyzing nuclei counter [Liu *et al.* (1984); Porstendörfer *et al.* (1985)] and of a noncontinuous expansion type CNC [Helsper and Nießner (1985)].

Some work has also been done with fluorinated hydrocarbons [e.g., see McDermott *et al.* (1991)]. However, the cost of continuous operation with this type of fluid is often prohibitive [Parsons and Mavliev (2001)]. Glycerol has been used as the condensing fluid in the particle growth system (PGS), which was tested for particles in the 3.9–70 nm size range [e.g., Rebours *et al.* (1996)]. However, no systematic study of a wide range of fluids has been found in the literature.

For CNLSD detection, an ability to detect smaller and smaller particles generally translates into an ability to detect lower and lower concentrations of analyte (assuming that nonvolatile background material in the buffer or mobile phase is not a limiting factor). This is especially true for CE–ES–CNLSD, where empirical data [Magnusson (2002)] indicate that the LOD of the system is limited partly by the inability of the best commercially available CNCs, i.e., the TSI UCPC 3025A, to grow and detect particles smaller than about 3 nm in diameter [Stolzenburg and McMurry (1991); Kesten *et al.* (1991)]. Thus, the sensitivity of CE–ES–CNLSD is limited by the UCPC size threshold for particle detection. It should be mentioned that Wiedensohler *et al.* (1997) reported a size threshold as low as 2.0 nm for the TSI UCPC 3025A. However, the lower cutoff may have been biased because of the use of differential mobility analyzers (DMAs) unsuitable for generating monodisperse particles in this low-size range. Too low size thresholds may have been reported due to diffusion in these DMAs, as suggested elsewhere [Gamero-Castaño and Fernández de la Mora (2000)]. These authors note further that the issue is complicated by the fact that the particles generated in DMAs are generally charged, which facilitates condensation, and, in some cases (positive ions in dibutyl phthalate vapors) enables detection even of subnanometer nuclei. On the other hand, other investigators have reported lower-size limits of about 3.5 nm for TSI's UCPC 3025 A [Alofs *et al.* (1995)]. With these considerations and conflicting data in mind, the manufacturer claimed lower size threshold of about 3 nm for this particle counter, supported by theoretical calculations, is taken as the true threshold.

The limitation in size threshold has become increasingly important. For example, even if the size threshold could be

lowered only from about 3 to 2 nm, the volume or mass of the smallest detectable particle would be reduced by three to four fold. This would lead to instruments with improved capabilities, extending the sensitivity of CNCs to smaller particles, which would lead to improved sensitivity in CNLSD. It would also permit detection of smaller particles in scanning mobility particle sizer (SMPS) systems and other systems using CNCs.

1.3. Organization of Paper

In Sec. 2, the current scientific background for selecting of the working liquid for CNLSD is presented. The Kelvin diameter will be adopted as a suitable approximation for the size of critical embryos for heterogeneous vapor nucleation. The influence of physical and chemical properties on heterogeneous nucleation are discussed, and the predictions of critical supersaturation using nucleation theory are considered. In Sec. 3, critical vapor saturation as a limiting condition for the condensation growth of heterogeneous seeds is discussed. Section 4 contains the description of the method for choosing the best working fluid. Here the correlations of Kelvin diameter with the dielectric constant and dielectric constant with the bulk surface tension are introduced. Finally, the strategy for selection of the working liquid for CNLSD is summarized in Sec. 5.

2. Present Method

2.1. Kelvin Diameter

It is customary to identify the condition for growth of a nucleus into a drop as that when this growth proceeds without an activation barrier. This corresponds to the diameter of the critical embryo, given in the classical nucleation theory (CNT) by the Kelvin diameter, and, more in general, by the Nucleation theorem. This diameter decreases with an increasing saturation ratio, but only to a point, when the saturation ratio reaches a *critical value* (the saturation ratio where one droplet per cubic centimeter and second is formed by homogeneous nucleation from vapor), the working fluid in the UCPC will start to condense on itself, growing into detectable droplets, thus producing false particle counts. After the critical value is reached, the number of droplets grown by homogeneous nucleation increases exponentially with increased supersaturation. It is this onset of homogeneous nucleation that puts the size-threshold for instruments operated with *n*-butanol as the condensing fluid at about 3 nm.

The critical supersaturation is different for different fluids however [e.g., Heist and He (1994)], and homogeneous nucleation will thus occur at different saturation ratios depending on which condensing fluid is utilized. Measurement of the critical supersaturation as a function of temperature for various condensing fluids has been a large part of a significant number of articles published since the early to mid 1970s [e.g., Katz *et al.* (1975)] through the 1980s and 1990s [e.g., Dillmann and Meier (1991)]. The measurements have most often been made in order to test and/or develop theories for vapor nucleation, for which a consistent rigorous theory applicable to all cases has yet to be developed. In more recent years, with advancement in experimental equipment, it has become more popular to measure the vapor nucleation rate in lieu of critical supersaturation [e.g., Anisimov *et al.* (1998)]. Critical supersaturation data can often be extracted from nucleation rate data.

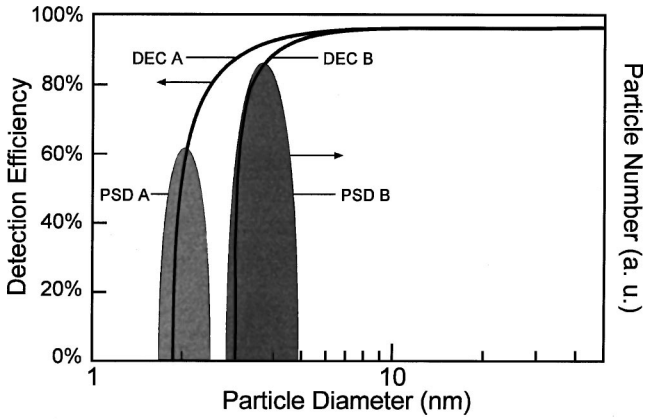

FIG. 1. The overlap of two detection efficiency curves, DEC-A having a size threshold of less than about 2 nm and DEC-B having a size threshold of about 3 nm, with two particle size distributions; PSD A for a lower analyte concentration PSD B for a higher analyte concentration. A CNC with DEC-A would grow and detect most of the particles in PSD A and virtually all of the particles in PSD B, while a CNC with DEC-B (e.g., TSI UCPC 3025A) would grow and detect most of the particles in PSD B, but none of the particles in PSD A.

The suitability or efficacy of a range of condensing fluids, for the purpose of growing particles as small as possible, can be evaluated by computing the Kelvin diameter based on published critical supersaturation data for each fluid. The Kelvin diameter depends not only on the saturation ratio, but also on surface tension, molecular weight, density, and temperature. Of these properties, surface tension and density are temperature dependent and measurements over various temperature ranges are available in the literature for many fluids. Up to this point, no systematic comparison of Kelvin diameters at critical supersaturation has been published for a wide range of fluids.

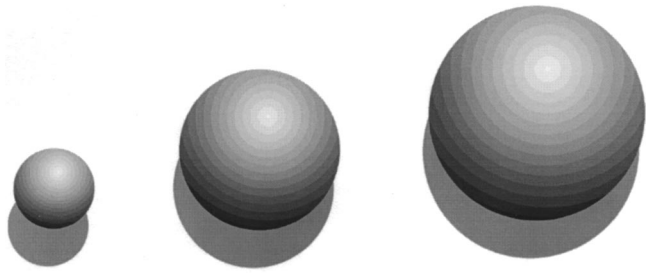

FIG. 2. A cartoon depiction of spherical particles having diameters of 1.5, 3.0, and 4.0 units, giving a visual idea of the difference in volume or mass of the particles that could be grown and detected using fluids with different Kelvin diameters for nanometer sizes.

However, two difficulties of using the Kelvin equation for calculation of the lower size threshold arise. Firstly, a few reports have found differences in detection efficiency based on the origin of the condensation nuclei. Both Helsper and Nießner (1985) and Porstendörfer *et al.* (1985) found differences in sensitivity between sodium chloride and silver particles in systems operating with water as the condensing fluid. Porstendörfer and co-workers [Porstendörfer *et al.* (1985)] suggested that the solubility of sodium chloride and the hydrophobicity of silver played a role in the findings. Some questions about the validity of these results exist, however, and even if the results are valid, no study of this effect exists for a range of fluids, i.e., it is not established that the effect is specific to water [e.g., see Rebours *et al.* (1996)]. Kesten *et al.* (1991) also found differences in detection efficiency of the *n*-butanol operated TSI UCPC 3025 for the same particle materials (silver and sodium chloride), but these differences were relatively small. It is logical to believe that the free energy barrier for condensation of a fluid onto a particle could be lowered under certain circumstances when some kind of attraction exists between the fluid and the particle, e.g., when the condensing fluid and the particle material are prone to reacting with one another [e.g., Magnusson *et al.* (1998)]. Perhaps the observed differences have to do with the charge state of the investigated particles. However, the available data are insufficient for establishing a good theoretical description of the phenomena [e.g., see Mavliev *et al.* (2001)].

On the other hand, close agreement with the Kelvin equation was found for condensation of water onto particles of dioctyl phtalate [Liu *et al.* (1984)]. Rebours *et al.* (1996) call the equation ''Kelvin's law'' in reference to the calculation of the size threshold. The results of McDermott *et al.* (1991) and of Stolzenburg and McMurry (1991), where the lower size threshold for growth and detection is accurately estimated using the Kelvin equation, should also be remembered. It may be that some of the discrepancies observed result from the same sources as the uncertainties in the determination of the lower size threshold, i.e., the use of DMA's unsuitable for this lower size range. However, it is not the goal of this research to explain the discrepancies observed by some authors, and the Kelvin equation is assumed to give an accurate estimation of the size threshold from the standpoint of condensation onto different particle materials.

The second difficulty concerns the fact that the Kelvin equation is based on the approximation of a spherical droplet and that macroscopic properties, such as the bulk liquid surface tension, are employed in the calculations. The validity of using macroscopic properties to describe highly curved surfaces with radii of curvature approaching molecular dimensions has been questioned [e.g., Everett and Haynes (1973); Melrose (1966), (1972), (1989)]. However, it has been found that the Kelvin equation holds to extraordinarily small radii of curvature, down to as small as one or two molecular diameters for simple liquids [e.g., see Hunter (1987)]. Measurements of forces of adhesion due to Laplace pressure in capillary-condensed cyclohexane between crossed mica cylinders have shown that major deviations from the Kelvin equation do not occur for meniscus radii above 0.5 nm, suggesting that macroscopic thermodynamics are in principle applicable to such small entities [Fisher and Israelachvili (1981); Fisher (1982)]. However, it was found at the same time that the situation is different for water, so that the Kelvin equation may not be applicable for low-nanometer sized water droplets. Further, Anisimov *et al.* (2001) used homogeneous nucleation rate data by Anisimov *et al.* (1998) to determine the excess energy of critical embryos for glycerol, using a method independent from the Kelvin equation. It was found that there are only slight differences in surface energy using this method compared to the Kelvin equation.

Most measurements to check the validity of the equation have been carried out in a three-phase (solid–liquid–vapor) system (i.e., the system of Fisher and Israelachvili), which means that the results obtained may be influenced by specific solid–liquid and solid–vapor interactions, contact angles and surface roughness, etc. Fenelonov *et al.* (2001) translated into English the article of Anisimov's group [Anisimov *et al.* (1978)]. Anisimov *et al.* (1978) used homogeneous nucleation experiments and concluded that the Kelvin equation is valid with an error not higher than 12%–14% for droplets of radii below 0.7–1.0 nm.

In the common case, the droplet approximation should be limited by the small size of clusters because the assumption that a small cluster can keep the bulk liquid density is unrealistic. Computer modeling of cluster formation from polar molecules shows that molecules form chains [''polymers,'' Rein ten Wolde *et al.* (1999)]. ''As the cluster size is increased, the polymers become longer. But, beyond a certain size, the clusters collapse to form a compact globule.'' This observation leads to the conclusion that critical embryos are represented by molecular chains up to at least 100 molecules. One hundred or more molecules collapse to globule form [Rein ten Wolde *et al.* (1999)]. A globule is closer to the droplet approximation. An impression of Kelvin equation validity arises because the surface excess energy and the cluster density go down simultaneously, with diminishing of the cluster molecule contents, even if the surface tension is reduced faster than it follows from the droplet approximation [Anisimov *et al.* (2001)].

In this study we compute Kelvin diameters at the critical supersaturation as a function of temperature for 30 different condensing fluids. The goal or this exercise is to identify the most promising fluids to use in techniques based on condensation nucleation processes, e.g., CNLSD, in order to grow and detect as small particles as possible, and thus increase the sensitivity of the detector. Another goal is to provide rational criteria for choosing the best fluid, even when e.g., critical supersaturation data are unavailable.

The Kelvin diameters are calculated based on published data for critical supersaturations, surface tensions, molecular weights and densities. Kelvin diameters based on critical supersaturation predicted by the CNT are also reported, as well

as calculations based on the nucleation theorem. The Kelvin diameters for different fluids are then compared and a new semiempirical method for predicting the best fluid, within a class of fluids, for growing the smallest particles is devised. This method is based upon the relative dielectric constant within the class of fluids [see also Koropchak *et al.* (2000)].

2.2. Extraction and Prediction of Data

A literature review was conducted to identify data for the variation with temperature of critical supersaturation, surface tension and density for most fluids available from the scientific literature. Inorganic materials except water were not considered due to e.g., unsuitable volatility properties for use in CNLSD.

The fluids for which sufficient data were found and which were taken for theoretical evaluation were *n*-nonane, Freon 11, *n*-hexane, *n*-octane, *n*-heptane, isopropanol, *n*-pentanol, propylene glycol, *n*-butanol, carbon tetrachloride, *n*-propanol, *o*-xylene, ethanol, *n*-butylbenzene, toluene, chloroform, methanol, heptanoic acid, 1,1,2,2-tetrachloroethane, trimethylene glycol, ethylene glycol, myristic acid, decanoic acid, glycerol, water, acetic acid, acetonitrile, benzonitrile, nitromethane, and nitrobenzene. The properties of the fluids, given as functions of temperature, are listed in Table 1.

2.3. Surface Tension

Jasper (1972) reviewed and published surface tension data for a wide range of pure liquid compounds. Data from Jasper were used for ethylene glycol, trimethylene glycol, *o*-xylene, toluene, *n*-butylbenzene, heptanoic acid, chloroform, carbon tetrachloride, and 1,1,2,2-tetrachloroethane. Data for *n*-heptane, *n*-hexane, *n*-nonane and *n*-octane were obtained from Jasper and Kring (1955); for *n*-butanol, ethanol, methanol, *n*-pentanol and *n*-propanol from Strey and Schmeling (1983); for isopropanol from Lide (1994); for glycerol from Vargaftik (1975); for water from Vargaftik *et al.* (1983); for Freon 11 from Heide (1973), and for decanoic acid from Hunten and Maass (1929). For acetic acid and propylene glycol, the equations given by Heist *et al.* (1976) and Kane *et al.* (1996), respectively, were used. For acetonitrile, benzonitrile, nitromethane, and nitrobenzene, equations given by Wright *et al.* (1993) were used. For myristic acid, an estimated equation given by Agarwal and Heist (1980) was used. In the cases where the authors did not provide equations, the given data were fit to third degree polynomials, or to straight lines using the method of least squares.

The surface tension equations are only valid within limited temperature ranges. Extrapolation outside the range where data were actually collected was avoided as much as possible, but for chloroform, the line was extrapolated down to 220 K, while the equation had been fit to data collected from 288 K and higher. For carbon tetrachloride, the line was extrapolated down to 260 K, while the equation had been fit to data collected from 288 K and higher. For Freon 11, the line was extrapolated down to 220 K, while the equation had been fit to data collected from 233 K and higher. For *n*-butanol, the line was extrapolated slightly above the highest data point (up to 320 K, while data were collected up to 313 K). The surface tension equations and their valid temperature ranges (when known) are also listed in Table 1.

2.4. Density

Data for methanol, and chloroform were obtained from *The International Critical Tables* (1928). Data for water, *n*-nonane, and *n*-butylbenzene were obtained from *Selected Values of Properties of Hydrocarbons and Related Compounds* (1965); for *n*-heptane, *n*-hexane and *n*-octane from Lide (1994), for glycerol from Vargaftik (1975), for *o*-xylene and toluene from Hales and Townsend (1972), and for ethanol, *n*-butanol, *n*-pentanol, *n*-propanol, isopropanol and myristic acid from Costello and Bowden (1958). The equation for heptanoic acid was estimated as the average of those for hexanoic and octanoic acids given by Costello and Bowden (1958). The last four references give experimental density data for a range of temperatures, and the data were fit to third degree polynomials using the method of least squares. Data for acetic acid were obtained from Timmermans (1950) and data for decanoic acid were obtained from Hunten and Maass (1929), and these data were fit to straight lines using linear regression. The equations for ethylene glycol, propylene glycol, and trimethylene glycol are estimated equations and were used as given by Kane and El-Shall (1996). For carbon tetrachloride, Freon 11, and 1,1,2,2-tetrachloroethane, equations as given by Katz *et al.* (1976) were used. For acetonitrile, benzonitrile, nitromethane, and nitrobenzene, equations given by Wright *et al.* (1993) were used.

Extrapolation of the lines outside the ranges where the data were actually collected was avoided. The valid temperature ranges for the density data for carbon tetrachloride, Freon 11, and 1,1,2,2-tetrachloroethane were not known. In these cases, it was assumed that the data are valid in the same range as the data for critical supersaturation. The density equations and their valid temperature ranges (when known) are also listed in Table 1.

2.5. Saturation Vapor Pressure

The saturation vapor pressure, p_s, is needed in theoretical estimations of the critical supersaturation ratio. Since the saturation vapor pressure usually is a required parameter in nucleation experiments, expressions for the temperature dependence of the saturation vapor pressure are usually reported in the articles concerning the measurement of critical supersaturation and/or nucleation rate. These equations are commonly given in the Antoine form, but sometimes in the Clausius–Clapeyron or another form.

The equations for acetic acid, *n*-butanol, ethanol, ethylene glycol, glycerol, isopropanol, methanol, *n*-propanol, propylene glycol and trimethylene glycol were obtained from Yaws (1994) and for *n*-pentanol from Anisimov *et al.* (2000). The equation for water was adapted from the *IAPWS Industrial Formulation 1997 for the Thermodynamic Properties of*

TABLE 1. Density (ρ), surface tension (σ), critical supersaturation (S_{cr}), and saturation vapor pressure (p_s) for the investigated fluids (references are given in the text)

acetic acid
$M = 60.05\ \mathrm{g\cdot mol^{-1}}$
$\rho = 1.0716 - 1.0914\cdot 10^{-3}\ t\ \mathrm{g\cdot cm^{-3}}$ (20–70 °C)
$\sigma = 29.427 - 0.0952\ t\ \mathrm{dyn\cdot cm^{-1}}$
$\ln S_{cr} = 6.699\cdot 10^{-7}\ T^3 - 6.934\cdot 10^{-4}\ T^2 + 0.2204\ T - 20.33$ (290–335 K)
$\log_{10} p_s = 28.3756 - 2973.4/T - 7.032\cdot \log T - 1.5051\cdot 10^{-9}\ T + 2.1806\cdot 10^{-6}\ T^2$ mm Hg (290–593 K)

***n*-butanol**
$M = 74.122\ \mathrm{g\cdot mol^{-1}}$
$\rho = -5.245\cdot 10^{-9}\ t^3 - 2.621\cdot 10^{-7}\ t^2 - 7.269\cdot 10^{-4}\ t + 0.8237\ \mathrm{g\cdot cm^{-3}}$ (−60–180 °C)
$\sigma = 25.98 - 0.08181\ t\ \mathrm{dyn\cdot cm^{-1}}$ (−35.10–39.90 °C)
$\ln S_{cr} = -2.912\cdot 10^{-7}\ T^3 + 3.059\cdot 10^{-4}\ T^2 - 0.1147\ T + 15.88$ (230–330 K)
$\log_{10} p_s = 39.6673 - 4001.7/T - 10.295\cdot \log T - 3.2572\cdot 10^{-10}\ T + 8.6672\cdot 10^{-7}\ T^2$ mm Hg (184–563 K)

***n*-butylbenzene**
$M = 134.212\ \mathrm{g\cdot mol^{-1}}$
$\rho = 4.434599\cdot 10^{-11}\ t^3 - 1.846525\cdot 10^{-7}\ t^2 - 8.036903\cdot 10^{-4}\ t + 0.87632\ \mathrm{g\cdot cm^{-3}}$ (−80–150 °C)
$\sigma = 31.28 - 0.1025\ t\ \mathrm{dyn\cdot cm^{-1}}$ (10–100 °C)
$\ln S_{cr} = -1.041\cdot 10^{-6}\ T^3 + 1.089\cdot 10^{-3}\ T^2 - 0.3953\ T + 51.24$ (220–360 K)
$\log_{10} p_s = 6.9808 - 1577.008/(T - 71.819)$ mm Hg

carbon tetrachloride
$M = 153.82\ \mathrm{g\cdot mol^{-1}}$
$\rho = 1.63186 - 1.867\cdot 10^{-3}\ t - 8.914\cdot 10^{-7}\ t^2 - 2.943\cdot 10^{-9}\ t^3\ \mathrm{g\cdot cm^{-3}}$
$\sigma = 29.49 - 0.1224\ t\ \mathrm{dyn\cdot cm^{-1}}$ (15–105 °C)
$\ln S_{cr} = 2.083\cdot 10^{-5}\ T^3 - 1.685\cdot 10^{-2}\ T^2 + 4.522\ T - 400.4$ (260–280 K)
$\log_{10} p_s = 6.9339 - 1242.43/(t + 230)$ mm Hg

chloroform
$M = 119.38\ \mathrm{g\cdot mol^{-1}}$
$\rho = 1.52643 - 1.8563\cdot 10^{-3}\ t - 0.5309\cdot 10^{-6}\ t^2 - 8.81\cdot 10^{-9}\ t^3\ \mathrm{g\cdot cm^{-3}}$ (−53–55 °C)
$\sigma = 29.91 - 0.1295\ t\ \mathrm{dyn\cdot cm^{-1}}$ (15–75 °C)
$\ln S_{cr} = 2.496\cdot 10^{-6}\ T^3 - 1.696\cdot 10^{-3}\ T^2 + 0.3585\ T - 20.59$ (220–260 K)
$\log_{10} p_s = 6.90328 - 1163.03/(t + 227.4)$ mm Hg

decanoic acid (*n*-capric acid)
$M = 172.26\ \mathrm{g\cdot mol^{-1}}$
$\rho = 0.91778 - 7.7131\cdot 10^{-4}\ t\ \mathrm{g\cdot cm^{-3}}$ (31.9–140.1 °C)
$\sigma = 30.46 - 0.0762\ t\ \mathrm{dyn\cdot cm^{-1}}$ (31.9–151.2 °C)
$\ln S_{cr} = 3.962\cdot 10^{-7}\ T^3 - 3.736\cdot 10^{-4}\ T^2 + 0.09390\ T - 1.757$ (340–430 K)
$\log_{10} p_s = 7.9458 - 2203.2/(T - 106.4)$ mm Hg

ethanol
$M = 46.069\ \mathrm{g\cdot mol^{-1}}$
$\rho = -1.431\cdot 10^{-8}\ t^3 + 9.770\cdot 10^{-7}\ t^2 - 8.706\cdot 10^{-4}\ t + 0.8063\ \mathrm{g\cdot cm^{-3}}$ (0–200 °C)
$\sigma = 23.88 - 0.08807\ t\ \mathrm{dyn\cdot cm^{-1}}$ (−50.74–39.70 °C)
$\ln S_{cr} = -2.588\cdot 10^{-7}\ T^3 + 2.6205\cdot 10^{-4}\ T^2 - 0.09328\ T + 12.089$ (210–300 K)
$\log_{10} p_s = 23.8442 - 2864.2/T - 5.0474\cdot \log T - 3.7448\cdot 10^{-11}\ T + 2.7361\cdot 10^{-7}\ T^2$ mm Hg (159–516 K)

ethylene glycol
$M = 62.069\ \mathrm{g\cdot mol^{-1}}$
$\rho = 1.1347 - 0.1026\cdot 10^{-2}\ t - 0.7094\cdot 10^{-6}\ t^2\ \mathrm{g\cdot cm^{-3}}$ (7-116 °C)
$\sigma = 50.21 - 0.0890\ t\ \mathrm{dyn\cdot cm^{-1}}$ (20-140 °C)
$\ln S_{cr} = 3.312\cdot 10^{-7}\ T^3 - 3.094\cdot 10^{-4}\ T^2 + 0.08932\ T - 6.036$ (284–362 K)
$\log_{10} p_s = 82.4062 - 6347.2/T - 25.433\cdot \log T - 2.3732\cdot 10^{-9}\ T + 8.7476\cdot 10^{-6}\ T^2$ mm Hg (260–645 K)

Freon 11 (CCl_3F)
$M = 137.38\ \mathrm{g\cdot mol^{-1}}$
$\rho = 2.05059 - 1.34278\cdot 10^{-3}\ T - 3.81417\cdot 10^{-6}\ T^2 + 1.10719\cdot 10^{-8}\ T^3 - 1.62766\cdot 10^{-11}\ T^4\ \mathrm{g\cdot cm^{-3}}$
$\sigma = 21.07 - 0.1256\ t\ \mathrm{dyn\cdot cm^{-1}}$ (−40–100 °C)
$\ln S_{cr} = 4.541\cdot 10^{-5}\ T^3 - 3.040\cdot 10^{-2}\ T^2 + 6.759\ T - 497.0$ (215–232.5 K)

glycerol
$M = 92.095\ \mathrm{g\cdot mol^{-1}}$
$\rho = 1267.414 - 0.317869\ t - 2.810384\cdot 10^{-3}\ t^2 - 2.751878\cdot 10^{-7}\ t^3\ \mathrm{kg\cdot m^{-3}}$ (20–240 °C)
$\sigma = 59.8933\cdot 10^{-3} - 1.62217\cdot 10^{-5}\ t - 4.61913\cdot 10^{-7}\ t^2 + 5.15906\cdot 10^{-10}\ t^3\ \mathrm{N\cdot m^{-1}}$ (20–150 °C)

TABLE 1. Density (ρ), surface tension (σ), critical supersaturation (S_{cr}), and saturation vapor pressure (p_s) for the investigated fluids (references are given in the text)—Continued

$\ln S_{cr} = -9.868\cdot10^{-6}\ T^3 + 9.324\cdot10^{-3}\ T^2 - 2.961\ T + 319.5$ (283–331 K)
$\ln S_{cr} = -1.167\cdot10^{-6}\ T^3 + 1.308\cdot10^{-3}\ T^2 - 0.4983\ T + 67.26$ (320.1–390.3 K)
$\log_{10} p_s = -62.7929 - 3658.5/T + 34.249\cdot\log T - 0.05194\ T + 2.283\cdot10^{-5}\ T^2$ mm Hg (291–723 K)

_n_-heptane
$M = 100.203\ \mathrm{g\cdot mol^{-1}}$
$\rho = \dfrac{100.203*10^{-3}}{0.16469\cdot10^{-2}\cdot0.26074^{(1+(1-T/540.26)^{2/7})}}\ \mathrm{kg\cdot m^{-3}}$ (183–538 K)
$\sigma = 22.10 - 0.0980\ t$ dyn·cm^{-1} (0–90 °C)
$\ln S_{cr} = -1.8255\cdot10^{-6}\ T^3 + 1.6270\cdot10^{-3}\ T^2 - 0.4993\ T + 54.071$ (250–285 K)
$p_s = 101.325\cdot\exp(1-371.552/T)\cdot\exp(2.8647 - 2.113204\cdot10^{-3}\ T + 2.250991\cdot10^{-6}\ T^2)$ kPa

heptanoic acid
$M = 130.19\ \mathrm{g\cdot mol^{-1}}$
$\rho = 0.9392 - 9.0180\cdot10^{-4}\ t\ \mathrm{g\cdot cm^{-3}}$ (20–280 °C)
$\sigma = 29.88 - 0.0848\ t$ dyn·cm^{-1} (15–70 °C)
$\ln S_{cr} = 1.120\cdot10^{-8}\ T^3 + 1.012\cdot10^{-5}\ T^2 - 0.02723\ T + 9.275$ (310–420 K)
$\log_{10} p_s = 8.352 - 2312.4/(T - 70.838)$ mm Hg

_n_-hexane
$M = 86.18\ \mathrm{g\cdot mol^{-1}}$
$\rho = \dfrac{86.18*10^{-3}}{0.14062\cdot10^{-2}\cdot0.26355^{(1+(T/507.43)^{2/7})}}\ \mathrm{kg\cdot m^{-3}}$ (183–500 K)
$\sigma = 20.44 - 0.1022\ t$ dyn·cm^{-1} (0–60 °C)
$\ln S_{cr} = 4.8928\cdot10^{-6}\ T^3 - 3.4888\cdot10^{-3}\ T^2 + 0.8020\ T - 57.051$ (225–265 K)
$\log_{10} p_s = 6.87776 - 1171.53/(T - 48.79)$ mm Hg

_n_-pentanol
$M = 88.149\ \mathrm{g\cdot mol^{-1}}$
$\rho = -4.9315\cdot10^{-9}\ t^3 + 2.8340\cdot10^{-7}\ t^2 - 7.3179\cdot10^{-4}\ t + 0.8276\ \mathrm{g\cdot cm^{-3}}$ (−60–180 °C)
$\sigma = 26.78 - 0.08147\ t$ dyn·cm^{-1} (−29.63–35.05 °C)
$\ln S_{cr} = -4.7360\cdot10^{-7}\ T^3 + 4.9890\cdot10^{-4}\ T^2 - 0.1841\ T + 24.436$ (240–320 K)
$p_s = \exp(90.08 - 9788/T - 9.9\cdot\ln T)$ mm Hg

isopropanol
$M = 60.09\ \mathrm{g\cdot mol^{-1}}$
$\rho = -4.6750\cdot10^{-9}\ t^3 - 5.1317\cdot10^{-7}\ t^2 - 7.5147\cdot10^{-4}\ t + 0.8169\ \mathrm{g\cdot cm^{-3}}$ (−60–160 °C)
$\sigma = 0.04445 - 0.7890\cdot10^{-4}\ T\ \mathrm{N\cdot m^{-1}}$ (283–353 K)
$\ln S_{cr} = 8.6551\cdot10^{-7}\ T^3 - 6.9165\cdot10^{-4}\ T^2 + 0.1735\ T - 12.404$ (270–310 K)
$\log_{10} p_s = 38.2363 - 3551.3/T - 10.031\cdot\log T - 3.474\cdot10^{-10}\ T + 1.7367\cdot10^{-6}\ T^2$ mm Hg (185–508 K)

_n_-propanol
$M = 60.069\ \mathrm{g\cdot mol^{-1}}$
$\rho = -1.3547\cdot10^{-8}\ t^3 + 1.3203\cdot10^{-6}\ t^2 - 8.6542\cdot10^{-4}\ t + 0.8200\ \mathrm{g\cdot cm^{-3}}$ (0–220 °C)
$\sigma = 25.28 - 0.08181\ t$ dyn·cm^{-1} (−29.99–44.31 °C)
$\ln S_{cr} = -9.1831\cdot10^{-8}\ T^3 + 1.1958\cdot10^{-4}\ T^2 - 0.05608\ T + 9.467$ (260–300 K)
$\log_{10} p_s = 31.5155 - 3457/T - 7.5235\cdot\log T - 4.287\cdot10^{-11}\ T + 1.3029\cdot10^{-7}\ T^2$ mm Hg (147–537 K)

myristic acid
$M = 228.38\ \mathrm{g\cdot mol^{-1}}$
$\rho = -1.668\cdot10^{-9}\ t^3 + 5.167\cdot10^{-7}\ t^2 - 7.462\cdot10^{-4}\ t + 0.9006\ \mathrm{g\cdot cm^{-3}}$ (60–300 °C)
$\sigma = 33.061 - 7.9836\cdot10^{-2}\ t$ dyn·cm^{-1} (76.2–119.2 °C)
$\ln S_{cr} = -7.308\cdot10^{-7}\ T^3 + 9.998\cdot10^{-4}\ T^2 - 0.4681\ T + 75.97$ (365–450 K)
$\log_{10} p_s = 8.2271 - 2536.2/(T - 114.5)$ mm Hg

methanol
$M = 32.042\ \mathrm{g\cdot mol^{-1}}$
$\rho = 0.81015 - 1.0041\cdot10^{-3}\ t - 1.802\cdot10^{-6}\ t^2 - 16.57\cdot10^{-9}\ t^3\ \mathrm{g\cdot cm^{-3}}$ (−94.5–15 °C)
$\rho = 0.80999 - 9.253\cdot10^{-4}\ t - 4.1\cdot10^{-7}\ t^2\ \mathrm{g\cdot cm^{-3}}$ (0–30 °C)
$\sigma = 24.23 - 0.09254\ t$ dyn·cm^{-1} (−47.40–37.10 °C)
$\ln S_{cr} = -3.602\cdot10^{-7}\ T^3 + 3.170\cdot10^{-4}\ T^2 - 0.09869\ T + 11.33$ (200–310 K)
$\log_{10} p_s = 45.6171 - 3244.7/T - 13.988\cdot\log T + 0.0066365\ T - 1.0507\cdot10^{-13}\ T^2$ mm Hg (175–513 K)

_n_-nonane
$M = 128.257\ \mathrm{g\cdot mol^{-1}}$

TABLE 1. Density (ρ), surface tension (σ), critical supersaturation (S_{cr}), and saturation vapor pressure (p_s) for the investigated fluids (references are given in the text)—Continued

$\rho = -3.577606\cdot10^{-9}\ t^3 + 3.000944\cdot10^{-7}\ t^2 - 7.874556\cdot10^{-4}\ t + 0.732697\ \mathrm{g\cdot cm^{-3}}$ (−53.75–260 °C)
$\sigma = 24.72 - 0.09347\ t\ \mathrm{dyn\cdot cm^{-1}}$ (10–120 °C)
$\ln S_{cr} = -6.706\cdot10^{-7}\ T^3 + 6.909\cdot10^{-4}\ T^2 - 0.2518\ T + 33.22$ (220–330 K)
$p_s = 101.325\cdot\exp(1-423.932/T)\cdot\exp(2.9469 - 2.051933\cdot10^{-3}\ T + 1.903683\cdot10^{-6}\ T^2)$ kPa

_n_-octane
$M = 114.230\ \mathrm{g\cdot mol^{-1}}$
$\rho = \dfrac{114.230*10^{-3}}{0.19122\cdot10^{-2}\cdot0.25678^{(1+(1-T/568.82)^{2/7})}}\ \mathrm{kg\cdot m^{-3}}$ (223–567 K)
$\sigma = 23.52 - 0.09509\ t\ \mathrm{dyn\cdot cm^{-1}}$ (0–100 °C)
$\ln S_{cr} = 2.5872\cdot10^{-7}\ T_3 - 5.6691\cdot10^{-5}\ T^2 - 0.05248\ T + 15.508$ (240–290 K)
$p_s = 101.325\cdot\exp(1-398.793/T)\cdot\exp(2.9015 - 2.046204\cdot10^{-3}\ T + 2.010759\cdot10^{-6}\ T^2)$ kPa

propylene glycol
$M = 76.096\ \mathrm{g\cdot mol^{-1}}$
$\rho = 1.069 - 1.1705\cdot10^{-3}\ t - 1.0045\cdot10^{-6}\ t^2\ \mathrm{g\cdot cm^{-3}}$ (−33–226 °C)
$\sigma = 41.18 - 0.099\ t\ \mathrm{dyn\cdot cm^{-1}}$ (30–60 °C)
$\ln S_{cr} = -9.636\cdot10^{-8}\ T^3 + 1.294\cdot10^{-4}\ T^2 - 0.05787\ T + 9.735$ (301.1–370.7 K)
$\log_{10} p_s = 90.293 - 6696.8/T - 28.109\cdot\log T - 1.3326\cdot10^{-10}\ T + 9.3651\cdot10^{-6}\ T^2$ mm Hg (213–626 K)

1,1,2,2-tetrachloroethane
$M = 167.85\ \mathrm{g\cdot mol^{-1}}$
$\rho = 1.62578 - 1.560\cdot10^{-3}\ t - 8.327\cdot10^{-8}\ t^2\ \mathrm{g\cdot cm^{-3}}$
$\sigma = 38.75 - 0.1268\ t\ \mathrm{dyn\cdot cm^{-1}}$ (15–105 °C)
$\ln S_{cr} = -7.744\cdot10^{-7}\ T^3 + 8.176\cdot10^{-4}\ T^2 - 0.3035\ T + 40.70$ (240–330 K)
$\log_{10} p_s = 7.0046 - 1444.3/(T - 68.05)$ mm Hg

toluene
$M = 92.134\ \mathrm{g\cdot mol^{-1}}$
$\rho = -4.59306\cdot10^{-9}\ T^3 + 4.25263\cdot10^{-6}\ T^2 - 2.25918\cdot10^{-3}\ T + 1.27950\ \mathrm{g\cdot cm^{-3}}$ (293.15–490 K)
$\sigma = 30.90 - 0.1189\ t\ \mathrm{dyn\cdot cm^{-1}}$ (10–100 °C)
$\ln S_{cr} = -1.101\cdot10^{-6}\ T^3 + 1.016\cdot10^{-3}\ T^2 - 0.3288\ T + 38.67$ (230–315 K)
$\log_{10} p_s = 6.95334 - 1343.943/(t + 219.377)$ mm Hg

trimethylene glycol
$M = 76.096\ \mathrm{g\cdot mol^{-1}}$
$\rho = 1.0775 - 0.8658\cdot10^{-3}\ t - 0.5248\cdot10^{-6}\ t^2\ \mathrm{g\cdot cm^{-3}}$ (33–227 °C)
$\sigma = 47.43 - 0.0903\ t\ \mathrm{dyn\cdot cm^{-1}}$ (20–140 °C)
$\ln S_{cr} = -7.880\cdot10^{-7}\ T^3 + 8.569\cdot10^{-4}\ T^2 - 0.3185\ T + 41.76$ (307.2–371.9 K)
$\log_{10} p_s = 27.4723 - 4020/T - 6.2839\cdot\log T - 6.7098\cdot10^{-10}\ T + 2.2952\cdot10^{-6}\ T^2$ mm Hg (246–658 K)

water
$M = 18.015\ \mathrm{g\cdot mol^{-1}}$
$\rho = 1.36832\cdot10^{-8}\ t^3 - 6.024554\cdot10^{-6}\ t^2 + 5.217572\cdot10^{-5}\ t + 0.999348\ \mathrm{g\cdot cm^{-3}}$ (−20–150 °C)
$\sigma = 235.8\cdot10^{-3}\left(\dfrac{647.13-T}{647.13}\right)^{1.256}\left(1 - 0.625\left(\dfrac{647.13-T}{647.13}\right)\right)\ \mathrm{N\cdot m^{-1}}$ (0–374 °C)
$\ln S_{cr} = -1.169\cdot10^{-7}\ T^3 + 1.574\cdot10^{-4}\ T^2 - 0.07361\ T + 12.28$ (250–350 K)
$p_s = \left[\dfrac{2C}{-B + (B^2 - 4AC)^{1/2}}\right]^4$ MPa (273.15–647.096 K),
where
$A = \vartheta^2 + 0.11670521452767\cdot10^4\cdot\vartheta - 0.72421316703206\cdot10^6$
$B = -0.17073846940092\cdot10^2\cdot\vartheta^2 + 0.12020824702470\cdot10^5\cdot\vartheta - 0.32325550322333\cdot10^7$
$C = 0.14915108613530\cdot10^2\cdot\vartheta^2 - 0.48232657361591\cdot10^4\cdot\vartheta + 0.40511340542057\cdot10^6$
$\vartheta = T + \dfrac{-0.23855557567849}{T - 0.65017534844798\cdot10^3}$

***o*-xylene**
$M = 106.160\ \mathrm{g\cdot mol^{-1}}$
$\rho = -2.86768\cdot10^{-9}\ T^3 + 2.56876\cdot10^{-6}\ T^2 - 1.61819\cdot10^{-3}\ T + 1.120607\ \mathrm{g\cdot cm^{-3}}$ (293.15–490 K)
$\sigma = 32.51 - 0.1101\ t\ \mathrm{dyn\cdot cm^{-1}}$ (10–100 °C)
$\ln S_{cr} = -2.071\cdot10^{-6}\ T^3 + 1.980\cdot10^{-3}\ T^2 - 0.6488\ T + 74.44$ (270–340 K)
$\log_{10} p_s = 6.99891 - 1474.679/(T - 59.464)$ mm Hg

Water and Steam (1997). The Antoine equation was used with constants obtained from Felder and Rousseau (1986) for carbon tetrachloride, chloroform, and toluene. The equations for *n*-heptane, *n*-nonane, and *n*-octane were used as given by Rudek *et al.* (1996) and the equation for *n*-hexane was used as given by Katz (1970). For the longer-chain carboxylic acids, the equations given by Agarwal and Heist (1980) were used and for 1,1,2,2-tetrachloroethane, the equation as given by Katz *et al.* (1976) was used. The equations for acetonitrile, benzonitrile, nitrobenzene, and nitromethane were used as given by Wright *et al.* (1993). The saturation vapor pressure equations are listed in Table 1.

2.6. Experimental Critical Supersaturation

Critical supersaturation is defined as the saturation ratio where the rate of nucleation, J, is 1 drop$\cdot$cm$^{-3}\cdot$s^{-1}. Experimental critical supersaturation has been measured and published in scientific literature for various fluids, with estimated overall errors of a few percent, generally up to 5%, while the error may be larger in some cases. Significant errors may be introduced because of the lack of accurate thermodynamic and hydrodynamic data needed to calculate supersaturation profiles within the cloud chambers used in the experiments. This is especially true for more ''uncommon'' fluids, such as the longer-chain carboxylic acids [e.g., Agarwal and Heist (1980)], and for 1,1,2,2-tetrachloroethane [Katz *et al.* (1976)], for which for example, vapor pressure data had to be roughly estimated by the authors.

Most of the experimental critical supersaturation data used in this research were obtained by manual extraction from plots of critical supersaturation versus temperature, published by various authors: for *o*-xylene, toluene, and *n*-butylbenzene by Katz *et al.* (1975); for chloroform, carbon tetrachloride, Freon 11, and 1,1,2,2-tetrachloroethane by Katz *et al.* (1976); for *n*-heptane, *n*-hexane and *n*-octane from Katz (1970); for acetic acid by Heist *et al.* (1976); for myristic, heptanoic, and decanoic acid by Agarwal and Heist (1980); for *n*-butanol, water, methanol, ethanol, *n*-propanol, and *n*-nonane by Dillmann and Meier (1991), for acetonitrile, benzonitrile, nitromethane, and nitrobenzene by Wright *et al.* (1993) and for isopropanol by Heist (1995). The data extracted from Dillmann and Meier (1991) were taken from their theoretical lines, which were shown to agree well with experimental points from various researchers. Data for ethylene glycol, propylene glycol, trimethylene glycol, and glycerol were obtained from Kane and El-Shall (1996), who gave their data in tables, so extraction from graphs was not necessary. Glycerol data from Anisimov *et al.* (1998) and *n*-pentanol data from Anisimov *et al.* (2000) were obtained from plots of nucleation rate versus vapor activity (supersaturation ratio for binary systems) at various temperatures and 0.10 MPa total pressure. The vapor activity at a nucleation rate of 1 drop$\cdot$cm$^{-3}\cdot$s^{-1} was used as the critical supersaturation. All supersaturation data were then fit to polynomials of the third degree, using the method of least squares, in the form

$$\ln S_{\mathrm{cr}} = aT^3 + bT^2 + cT + d,$$

where S_{cr} is the critical supersaturation; a, b, c, and d are regression coefficients; and T is the temperature in Kelvin (K). Table 1 contains the equations and valid temperature ranges for the investigated fluids while the data are shown as graphs in Fig. 3. Of the data presented, those for carboxylic acids are probably among the least accurate, for the reasons described above.

2.7. Prediction of Critical Supersaturation from Theory

The CNT gives the rate of nucleation of a supersaturated vapor, J (drops$\cdot$cm$^{-3}\cdot$s^{-1}), as an Arrhenius-type relation

$$J = C \cdot e^{(-\Delta F^*/RT)},$$

where the kinetic coefficient C was derived by Becker and Döring (1935). The expression becomes

$$J = \frac{q}{\rho}\sqrt{\frac{2N_{\mathrm{A}}^3\sigma M}{\pi}}\left(\frac{Sp_{\mathrm{s}}}{RT}\right)^2 e^{(-\Delta F^*/RT)},$$

where q is a sticking coefficient, which is set equal to 1 [e.g., Wright *et al.* (1993)], ρ is density, N_{A} is Avogadro's number, σ is surface tension, M is molecular weight, S is supersaturation, and p_{s} is the saturation vapor pressure for the vapor. In the exponent, ΔF^* is the maximum of the rise, ΔF, in free energy as a spherical embryo of diameter d is formed isothermally and isobarically

$$\Delta F = \pi d^2\sigma - \frac{\rho\pi d^3}{6M}RT\ln S.$$

The first term on the right is the contribution of the surface free energy and the second term is the contribution to ΔF from the bulk free energy change [e.g., see McDonald (1962)]. The maximum is found by deriving ΔF with respect to d, setting equal to zero, and solving for d. This, of course, gives the Kelvin equation, which is then inserted into the expression for ΔF so that the maximum becomes

$$\Delta F^* = \frac{16\pi N_{\mathrm{A}}M^2\sigma^3}{3(\rho RT\ln S)^2}.$$

If J is set equal to 1 drop$\cdot$cm$^{-3}\cdot$s^{-1}, and the literature values for the surface tension, density, and saturation vapor pressure are used (Table 1), the critical supersaturation, $S_{\mathrm{cr(CNT)}}$ can be predicted as a function of temperature by solving the nucleation rate equation for S. Thus, $S_{\mathrm{cr(CNT)}}$ can be predicted from macroscopic fluid properties.

A computer program, CNT predictor, was used for processing the macroscopic data and to output the predicted $S_{\mathrm{cr(CNT)}}$ data in files suitable for input into a spread sheet for processing and graphing. The equation for $J=1$ drop$\cdot$cm$^{-3}\cdot$s^{-1} was solved numerically within CNT predictor using the method of Newton–Raphson [e.g., Ekbom (1991)]. The accuracy of the results was verified by comparison to CNT predictions published by various authors. Figure 4 shows the natural logarithm of the predicted critical supersaturation versus temperature for the investigated fluids, excluding Freon 11.

3. Results and Discussion

3.1. Critical Supersaturation, Comparison to CNT

The experimental critical supersaturation data for all of the investigated fluids are shown graphically in Fig. 3. This figure probably represents one of the most comprehensive compilations of experimental critical supersaturation versus temperature to date. The critical supersaturation data predicted using the CNT over the same temperature ranges as the experimental data are shown in Fig. 4. The CNT has been found to describe the nucleation of many fluids fairly well, while significant errors are found for other fluids [e.g., see Kane and El-Shall, (1996)]. Taking the experimentally determined critical supersaturation as the true value, the relative error of using the CNT for prediction of the same can be evaluated. Table 2 lists the investigated fluids and the arithmetic average of the percent relative error, over the present temperature range, of using the CNT for prediction of the critical supersaturation. Figure 5 shows the data in graphical form. Using the median instead of the arithmetic average did not significantly change the result in any case. In view of the estimated errors for experimental critical supersaturation data sometimes being as high as 8% or more, the fluids can be divided into three groups, namely those fluids for which the predicted critical supersaturation is too low (lower than about −10% relative error), those fluids for which the CNT predicts the critical supersaturation fairly well (within the range of −10% to +10% relative error) and those fluids for which the prediction gives too high values (more than about +10% relative error). The first group includes fluids such as benzonitrile, acetic acid, acetonitrile, glycerol [from Kane and El-Shall, (1996)] and nitromethane. The second group includes fluids such as methanol, chloroform, *n*-heptane, toluene, ethanol, *n*-hexane, water, carbon tetrachloride, *n*-propanol, isopropanol, *n*-octane, heptanoic acid, 1,1,2,2-tetrachloroethane, *n*-butanol, and *o*-xylene. The third group includes the fluids *n*-pentanol, glycerol [from Anisimov *et al.* (1998)], trimethylene glycol, myristic acid, propylene glycol, and *n*-nonane. The average percent relative error for ethylene glycol, *n*-butylbenzene, and decanoic acid is quite small, but the variation is large over the temperature range, especially for ethylene glycol. For the latter, the error is positive at lower temperatures and becomes negative at higher temperatures. For *n*-butylbenzene, the error is slightly positive at lower temperatures and becomes negative at the higher temperatures, while the error is negative at lower temperatures and slightly positive at higher temperatures for decanoic acid. It is also interesting to note that there is a considerable difference in the data for glycerol obtained by Kane and El-Shall, compared to the data of Anisimov *et al.* (1998). Of these, the data from Anisimov's group seem to have a slope more consistent with the majority of the experimental critical supersaturations and Kelvin diameters for other fluids reported by other authors and are believed have more physical meaning. Acetic acid, with the maximum relative error being about +92%, also deserves special mention. The large discrepancy was ascribed by Agarwal and Heist (1980) to significant association of acetic acid molecules in the vapor phase.

3.2. Kelvin Diameters at Critical Supersaturation

With knowledge of the critical supersaturation, the Kelvin diameter at critical supersaturation as a function of temperature can be calculated as

$$d_{\mathrm{K,Scr}}=\frac{4\sigma M}{\rho RT\ln S_{\mathrm{cr}}}.$$

The data in Table 1 were converted to SI units and the Kelvin equation was used to calculate the respective Kelvin diameters over the valid temperature ranges. Calculations were done using both the experimental and predicted critical supersaturation. Based on the estimated errors in experimental critical supersaturation given by the various authors, and assuming that the critical supersaturation is the most uncertain parameter in the Kelvin equation, the percent relative error in the Kelvin diameter calculated from experimental critical supersaturation should be less than 5% in most cases and not over about 10% in any case. The results can be seen in Figs. 6 and 7, respectively. These figures show the calculated Kelvin diameters versus temperature for the different investigated fluids. As Fig. 3, Fig. 6 has two lines for glycerol: line 24 is based on critical supersaturation data obtained from Anisimov *et al.* (1998), while line 26 is based on data obtained from Kane and El-Shall (1996).

As can be seen in Figs. 6 and 7, and taking the Kelvin diameter calculated from experimental supersaturation as the true value, the Kelvin diameters calculated based on experimental critical supersaturation and the CNT-predicted critical supersaturation agree fairly well for many of the fluids (mirroring the errors in critical supersaturation). However, the relative errors are somewhat smaller due to the natural logarithm of supersaturation in the Kelvin equation. Nevertheless, the relative errors are still large in several cases and the internal order between the calculated Kelvin diameters is quite different for the two cases. Table 3 shows the Kelvin diameters at a temperature of 300 K calculated from experimental data and from CNT, ordered from the smallest to the largest numerical value. Note that the number caption associated with each fluid in this table is different from the numbers used in the figures. The temperature of 300 K was chosen to minimize the need for extrapolation. Data points were available for most fluids at this temperature and limited extrapolation was required only in a few cases, while longer extrapolations were required in a couple of cases. Freon 11 was excluded because the extrapolation would be unreasonably long for this fluid.

As seen in Table 3, the order between the Kelvin diameters is different for the two cases. However, both methods place glycerol, water, and benzonitrile among the fluids having the lowest Kelvin diameters, and the normal alkanes as having the highest Kelvin diameters. It is also interesting to note that the Kelvin diameter for the monohydroxylated alcohols in-

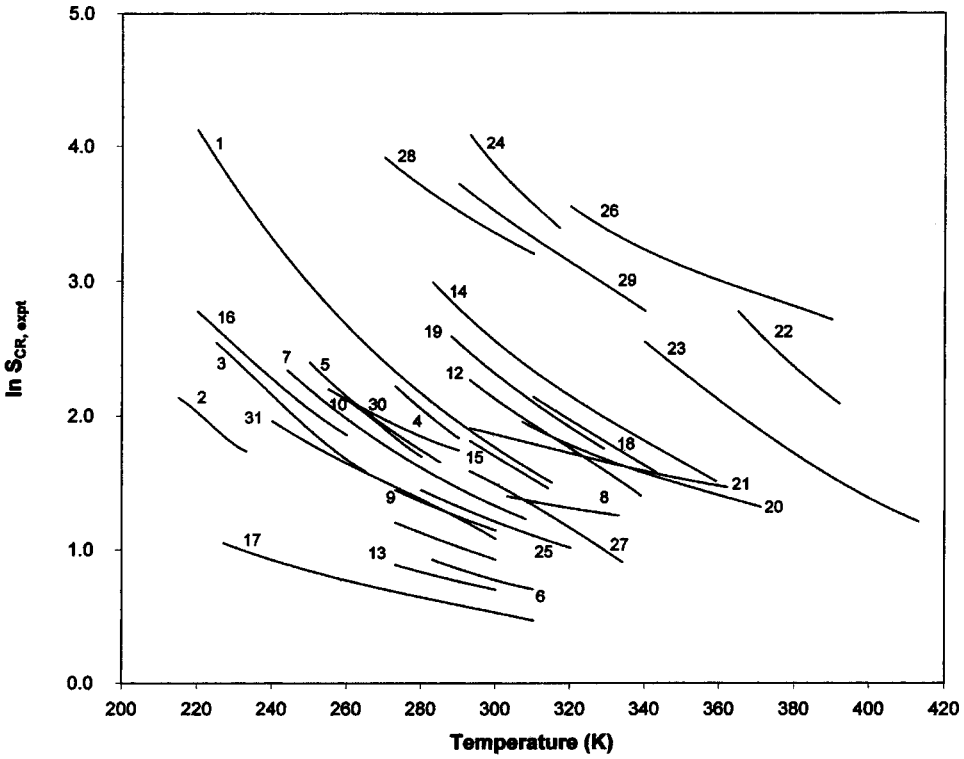

FIG. 3. Experimental critical supersaturation data for: (1) *n*-nonane, (2) Freon 11, (3) *n*-hexane, (4) *n*-octane, (5) *n*-heptane, (6) isopropanol, (7) *n*-pentanol, (8) propylene glycol, (9) *n*-butanol, (10) carbon tetrachloride, (11) *n*-propanol, (12) *o*-xylene, (13) ethanol, (14) *n*-butylbenzene, (15) toluene, (16) chloroform, (17) methanol, (18) heptanoic acid, (19) 1,1,2,2-tetrachloroethane, (20) trimethylene glycol, (21) ethylene glycol, (22) myristic acid, (23) decanoic acid, (24), (26) glycerol, (25) water, (27) acetic acid, (28) benzonitrile, (29) nitrobenzene, (30) nitromethane and (31) acetonitrile. Glycerol has two lines (24) and (26), based on data from two different sources.

creases with increasing carbon chain length when experimental supersaturation is used, while the opposite trend is seen when the CNT is used.

Figure 8 illustrates the Kelvin diameter determined from experimental data plotted versus the CNT-determined Kelvin diameter. As in Table 3, Freon 11 is excluded. This plot shows that the agreement between experimental and theoretical data is only moderate, with a squared correlation coefficient for a straight line of about 0.50. If the carboxylic acids are also excluded, the squared correlation coefficient is somewhat higher at about 0.60, which is still not more than a moderate correlation. Based on this plot, and because the difference between the CNT-determined Kelvin diameter and the Kelvin diameter determined from experimental data in several cases is significantly larger than the error estimated based on experimental uncertainties, the Kelvin diameters calculated based on experimentally determined critical supersaturation are believed to be generally more accurate. These are the ones that will be referred to in the further discussions, unless otherwise noted.

As seen in the figures above and in Table 3, acetic acid, glycerol, and water have the lowest Kelvin diameters (~1.5–2 nm) among the fluids in this investigation and will therefore be subjected to a somewhat more detailed discussion.

Based on the previously mentioned results of Fisher (1982) and Fisher and Israelachvili (1981), it is reasonable to believe that the Kelvin equation is applicable to the organic fluids acetic acid and glycerol, but it may be that the result for water is invalid. The result for acetic acid is questionable for other reasons, though. As already noted, the vapors of this fluid are known to be significantly associated [Heist *et al.* (1976)], i.e., most of the molecules are dimers, which would mean that the average apparent molecular weight is almost doubled from that of nonassociated acetic acid. This, in turn, means that the ''true'' Kelvin diameter may be quite different than the calculated value. Thus, acetic acid may not be a viable choice for use in CNCs (in addition to the problems that would arise from continual operation with a corrosive fluid).

The validity of the result for glycerol can be evaluated from a different perspective because of readily available nucleation rate data from Anisimov *et al.* (1998). This can be done by using an alternative method, by which the number of molecules in the critical embryo is calculated from nucleation rate data [e.g., see Anisimov *et al.* (1978), (1998)]

$$\left(\frac{\partial \ln J}{\partial \ln a}\right)_{T,P} = n^* + 2,$$

where n^* is the number of molecules in the critical embryo and a is the vapor activity (or supersaturation for a unary system). This relationship provides a method, independent from the Kelvin equation, to calculate the critical embryo size from the slope in plots of nucleation rate versus vapor activity (or supersaturation). If n^* is known, one can use density–volume relationships to predict the spherical diameter of such an embryo. This diameter can then be compared to the calculated Kelvin diameter. This approach is similar to that taken by Anisimov *et al.* (2001).

The number of molecules in the critical embryo was calculated for the case of glycerol based on the nucleation rate

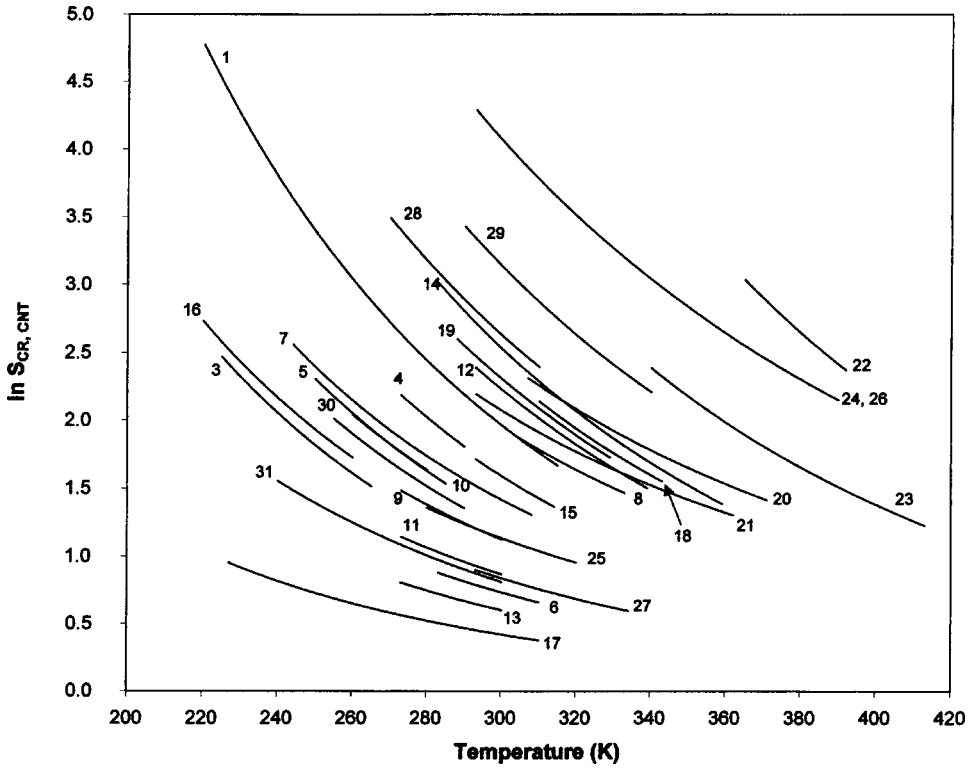

FIG. 4. Critical supersaturation predicted using classical nucleation theory for (1) *n*-nonane, (2) Freon 11, (3) *n*-hexane, (4) *n*-octane, (5) *n*-heptane, (6) isopropanol, (7) *n*-pentanol, (8) propylene glycol, (9) *n*-butanol, (10) carbon tetrachloride, (11) *n*-propanol, (12) *o*-xylene, (13) ethanol, (14) *n*-butylbenzene, (15) toluene, (16) chloroform, (17) methanol, (18) heptanoic acid, (19) 1,1,2,2-tetrachloroethane, (20) trimethylene glycol, (21) ethylene glycol, (22) myristic acid, (23) decanoic acid, (24), (26) glycerol, (25) water, (27) acetic acid, (28) benzonitrile, (29) nitrobenzene, (30) nitromethane and (31) acetonitrile.

data in Anisimov (1998) at a total pressure of 0.1 MPa and a rate of nucleation of 3000 drops$\cdot$cm$^{-3}\cdot$s^{-1}. The liquid density, molecular weight and Avogadro's number were then used to convert the number of molecules into droplet diameter. A plot of the calculated Kelvin diameter divided by the diameter calculated from the number of molecules in the critical embryo is shown in Fig. 9. The ''jumps'' at about 295 and 317 K are due to phase transitions in the critical embryo (see the reference for more information), and these points are disregarded in the following discussion. The number of molecules in the critical embryo range from about 9 to 34 in this temperature range, excluding the ''jumps.''

It can be seen in this figure that the percent relative error of using the Kelvin diameter (taking the diameter calculated from n^* as the true value) ranges from about (-13%) to $+23\%$, with an average of about $+2\%$ for the present temperature range. With the approximate nature of determining the slope from the nucleation rate in mind, this must be seen as a fairly reasonable agreement between the two methods of calculating the critical embryo size and lends additional support to the validity of using the Kelvin equation, at least for glycerol, for these small droplet diameters. Note further that the critical diameter obtained from the nucleation theorem is close to 1.4 nm at the lowest temperature for which glycerol data are shown in the figure.

The highest Kelvin diameters calculated, within reasonable temperature ranges, were over 4 nm for heptanoic acid. Normal butanol, which is frequently used as a condensing agent in commercial CNCs, has a Kelvin diameter of $\sim$2.8–3.3 nm, which is close to the size threshold for the best commercial CNCs in which *n*-butanol is used (i.e. TSI UCPC 3025A). Figure 10 shows the detection efficiency curve for the TSI UCPC 3025A, according to Kesten *et al.* (1991). The curve shown represents the average of the curves for silver and sodium chloride particles. As seen, the cutoff below which no particles can be detected lies at about 2.8 nm.

Again, several of the investigated fluids have Kelvin diameters that are lower than the one for *n*-butanol. This suggests that the size threshold for particle detection could be lowered, thus making the CNC more efficient for smaller particles, by choosing a condensing fluid that has a lower Kelvin diameter.

As mentioned earlier, lowering the temperature of the condenser in the CNC can decrease the threshold for particle detection because of the increase in supersaturation ratio. In addition, the Kelvin diameter is generally lower at lower nucleation temperature, which can also be seen in Fig. 6, where most of the lines for the Kelvin diameters have positive slopes, with the exception of benzonitrile, ethylene glycol, and propylene glycol, which have negative slopes. Glycerol [line 26, from Kane and El-Shall, (1996)] has both a positive and a negative slope in different temperature ranges, while glycerol data from Anisimov *et al.* (1998) has a positive slope over the full measured range. Nitromethane (line 30) also has both a positive and a negative slope. For ethylene glycol and propylene glycol, the critical supersaturation does not increase as much as it does for the other fluids with decreasing temperature, i.e., the slope is not as negative. This would indicate that the size threshold for these liquids could increase when the nucleation temperature is lowered. However, it should be remembered that the density data for eth-

TABLE 2. Arithmetic average of the percent relative error in critical supersaturation resulting from using the CNT, taking the experimentally determined critical supersaturation data as true

Fluid	Average relative error in Scr (%)	Range
n-hexane	−8.0	−9.9 to −5.9
n-heptane	−9.4	−11.1 to −8.6
n-octane	−2.6	−3.3 to −2.2
n-nonane	43.5	18.4 to 91.7
chloroform	−9.6	−11.9 to −4.6
1,1,2,2-tetrachloroethane	−0.95	−2.3 to 0.80
carbon tetrachloride	−7.0	−8.2 to −5.5
methanol	−10.6	−11.3 to −8.8
ethanol	−8.6	−9.4 to −7.7
n-propanol	−5.8	−5.9 to −5.6
n-butanol	0.86	−1.9 to 4.2
n-pentanol	15.0	8.2 to 24.5
trimetylene glycol	25.0	10.2 to 43.1
propylene glycol	42.5	23.7 to 64.9
ethylene glycol	3.4	−14.9 to 33.7
glycerol	22.6	20.3 to 25.8
glycerol 2	−26.0	−43.0 to −4.8
o-xylene	9.1	6.9 to 13.4
toluene	−9.4	−9.7 to −8.7
n-butylbenzene	−6.8	−12.0 to 1.68
benzonitrile	−46.2	−34.7 to −55.3
nitrobenzene	−36.9	−43.3 to −25.5
myristic acid	32.2	29.7 to 33.2
heptanoic acid	−2.5	−3.3 to 0.15
decanoic acid	−6.7	−14.9 to 2.0
acetic acid	−40.5	−49.6 to −26.6
water	−7.1	−8.5 to −5.7
2-propanol	−3.9	−4.5 to −3.7
acetonitrile	−30.8	−33.3 to −23.5
nitromethane	−24.8	−32.1 to −16.8

ylene glycol and propylene glycol were estimated by Kane and El-Shall (1996), and not actually measured over the full temperature range.

4. Method for Choosing the Best Fluid

4.1. Kelvin Equation

By calculating the Kelvin diameter for a wide range of fluids, it was found that glycerol and water are especially viable fluids for lowering the size threshold in a CNC. The calculation required knowledge of, among other data, the critical supersaturation. This parameter is not known experimentally for most fluids, and although it can be predicted using, e.g., the CNT, the calculations, while not too complicated, are quite tedious and many fluids do not follow the theory. Hence, it would be preferable to have a method by which the most efficient fluid could be quickly found, without the knowledge of such data. Thus, the following analyses were undertaken.

4.2. Analysis Based on the CNT—The Surface Tension

The CNT, although based on macroscopic fluidic properties and not on properties at the molecular level, has been quite helpful for the understanding of general nucleation phenomena. It can be seen from the CNT nucleation rate equation that the surface tension, σ, of the fluid plays an especially important role because it is in the exponent and then raised to the third power. There is no explicit solution for S in the CNT equation for nucleation rate, in its present form, when the rate, J, is set to 1. It is therefore not possible to introduce an explicit theoretical expression for the Kelvin equation. However, if the $S \cdot p_s$ factor is exchanged for the partial pressure, p, of the fluid vapor, it is possible to explicitly solve the equation for $\ln S$. The equation can then be written in the form

$$J = a e^{[-b/(\ln S)^2]},$$

where

$$a = \frac{1}{d}\sqrt{\frac{2N_A^3 \sigma M}{\pi}}\left(\frac{p}{RT}\right)^2$$

(not to be confused with vapor activity) and

$$b = \frac{16\pi N_A M^2 \sigma^3}{3\rho^2 R^3 T^3}.$$

Setting $J = 1\ \text{drop}\cdot\text{cm}^{-3}\cdot\text{s}^{-1}$ gives

$$\ln S = \sqrt{\frac{b}{\ln a}}$$

or

$$\ln S = -\sqrt{\frac{b}{\ln a}},$$

where the second solution is discarded because $\ln S$ must be greater than zero since S, being supersaturation, is by definition greater than unity. Since $J = 1\ \text{drop}\cdot\text{cm}^{-3}\cdot\text{s}^{-1}$, $\ln S_{cr} = \ln S$. The solution is then inserted into the Kelvin equation, which upon rearrangement becomes

$$d_{K,CNT,Scr} = \frac{\sqrt{6\,RT \ln \dfrac{2MN_A^3\sigma p^4}{\rho^2 \pi R^4 T^4}}}{2\sigma^{1/2}\sqrt{N_A \pi}}.$$

It is clear from this expression that the surface tension is the strongest factor that influences the theoretical Kelvin diameter as expressed by the CNT so that the theoretical Kelvin diameter is directly proportional to the square root of the reciprocal surface tension. This means that fluids having higher surface tension should generally give smaller theoretical Kelvin diameters and vice versa. Figure 11 shows the theoretical Kelvin diameter at a temperature of 300 K versus the square root of the reciprocal surface tension. As expected, the data adhere well to a straight line, with a squared correlation coefficient of about 0.98. Note that the data points for the carboxylic acids and Freon 11 are excluded from the plot because of long extrapolations being necessary to obtain the points and because of uncertainties in the data.

Figure 12 shows the Kelvin diameters determined from experimental critical supersaturation plotted versus the

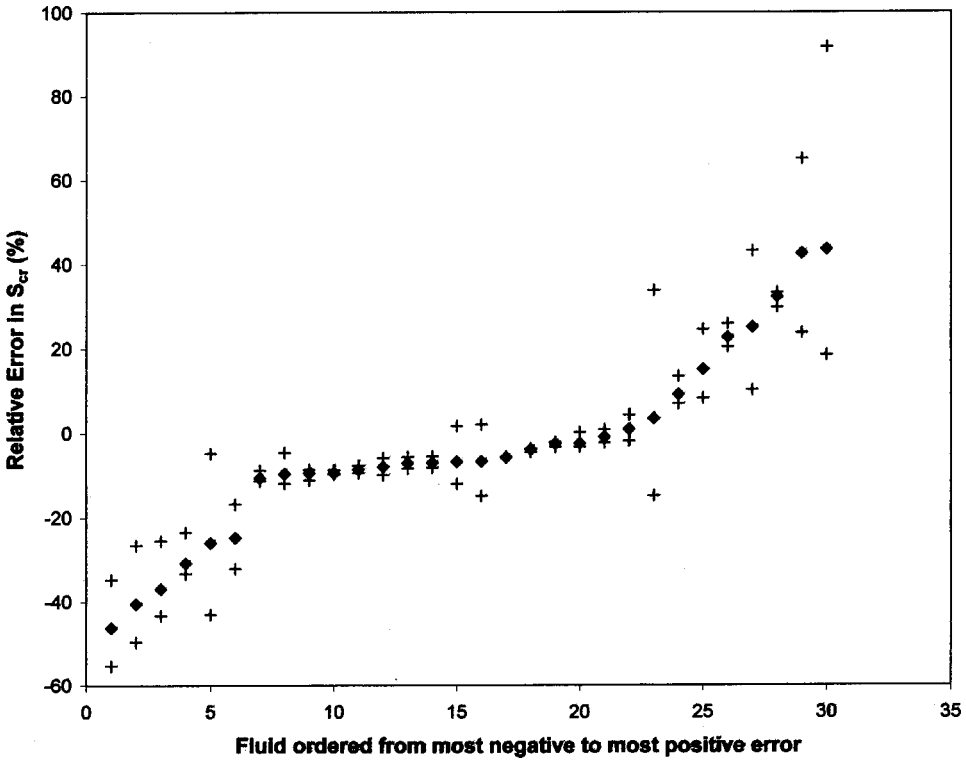

FIG. 5. Arithmetic average (filled diamonds) of the percent relative error of using the CNT to predict critical supersaturation, taking the experimentally determined critical supersaturation as true. The plus-symbols represent the lowest and highest values over the temperature range. The fluids are: (1) benzonitrile, (2) acetic acid, (3) nitrobenzene, (4) acetonitrile, (5) glycerol (Kane and El-Shall, 1996), (6) nitromethane, (7) methanol, (8) chloroform, (9) *n*-heptane, (10) toluene, (11) ethanol, (12) *n*-hexane, (13) water, (14) carbon tetrachloride, (15) *n*-butylbenzene, (16) decanoic acid, (17) *n*-propanol, (18) 2-propanol, (19) *n*-octane, (20) heptanoic acid, (21) 1,1,2,2-tetrachloroethane, (22) *n*-butanol, (23) ethylene glycol, (24) *o*-xylene, (25) *n*-pentanol, (26) glycerol (Anisimov, *et al.*, 1998), (27) trimetylene glycol, (27) myristic acid, (28) propylene glycol, (29) *n*-nonane. Note that the numbering of the fluids differs from that in Figs. 3 and 4.

square root of the reciprocal surface tension. The squared correlation coefficient for a linear regression of these data has a value of about 0.67, suggesting a moderate to fairly strong correlation between Kelvin diameter and the square root of the reciprocal surface tension. The trend for fluids with higher surface tensions having lower Kelvin diameters and vice versa is relatively clear. As before, the data points for the carboxylic acids and Freon 11 are excluded from the plot. A somewhat higher correlation is obtained when the Kelvin diameter data for experimental supersaturation are plotted versus the square root of $\ln(M\cdot\sigma)/\sigma$ (Fig. 13). The squared correlation coefficient is about 0.72 for a linear re-

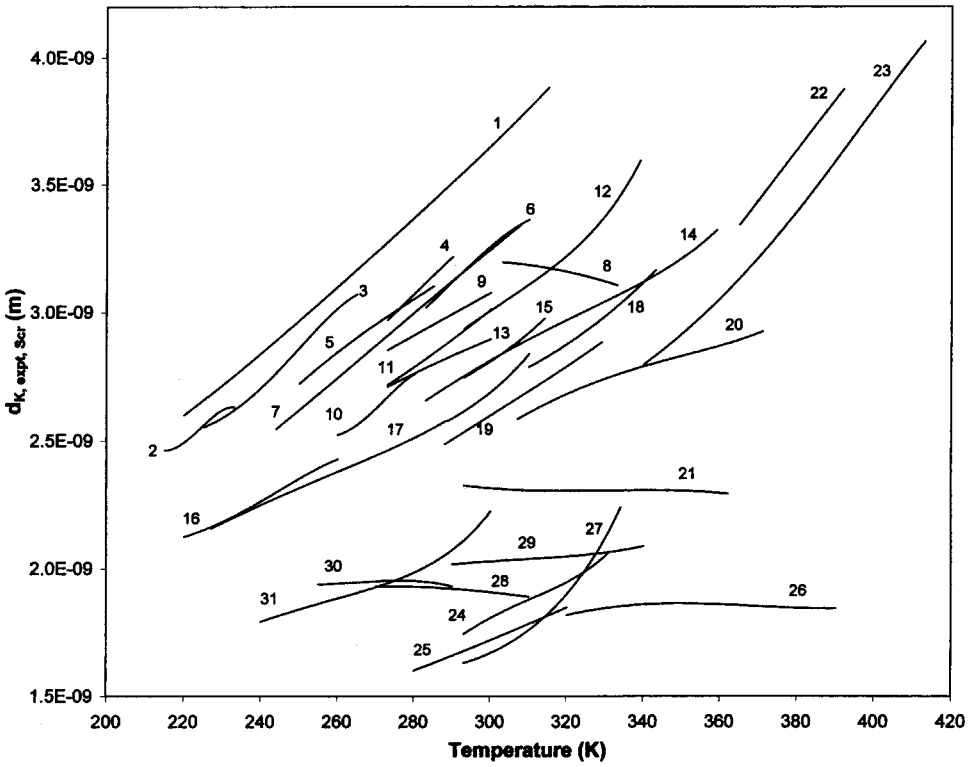

FIG. 6. Calculated Kelvin diameter from experimental critical supersaturation data for (1) *n*-nonane, (2) Freon 11, (3) *n*-hexane, (4) *n*-octane, (5) *n*-heptane, (6) isopropanol, (7) *n*-pentanol, (8) propylene glycol, (9) *n*-butanol, (10) carbon tetrachloride, (11) *n*-propanol, (12) *o*-xylene, (13) ethanol, (14) *n*-butylbenzene, (15) toluene, (16) chloroform, (17) methanol, (18) heptanoic acid, (19) 1,1,2,2-tetrachloroethane, (20) trimethylene glycol, (21) ethylene glycol, (22) myristic acid, (23) decanoic acid, (24, 26) glycerol, (25) water, (27) acetic acid, (28) benzonitrile, (29) nitrobenzene, (30) nitromethane and (31) acetonitrile. Glycerol has two lines (24) and (26) from two different sources.

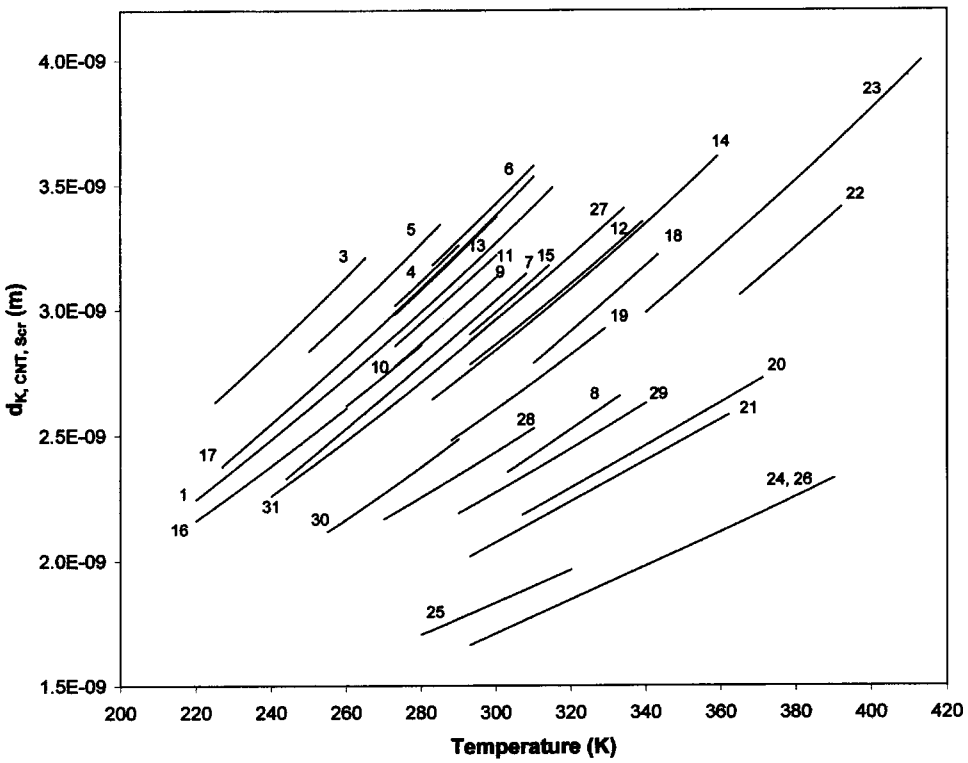

FIG. 7. Kelvin diameters calculated using classical nucleation theory for (1) *n*-nonane, (3) *n*-hexane, (4) *n*-octane, (5) *n*-heptane, (6) isopropanol, (7) *n*-pentanol, (8) propylene glycol, (9) *n*-butanol, (10) carbon tetrachloride, (11) *n*-propanol, (12) *o*-xylene, (13) ethanol, (14) *n*-butylbenzene, (15) toluene, (16) chloroform, (17) methanol, (18) heptanoic acid, (19) 1,1,2,2-tetrachloroethane, (20) trimethylene glycol, (21) ethylene glycol, (22) myristic acid, (23) decanoic acid, (24, 26) glycerol, (25) water, (27) acetic acid, (28) benzonitrile, (29) nitrobenzene, (30) nitromethane and (31) acetonitrile.

gression, which is slightly higher than the correlation obtained when plotting versus the square root of the reciprocal surface tension. Including the density does not significantly improve the correlation, mainly because most of the densities are close to unity and fairly similar for all of the fluids.

Again, these plots show that a fluid having a high surface tension (most important), in combination with a low molecular weight (of lesser importance) will generally have a lower Kelvin diameter. Using the surface tension alone or the surface tension and the molecular weight criteria together cor-

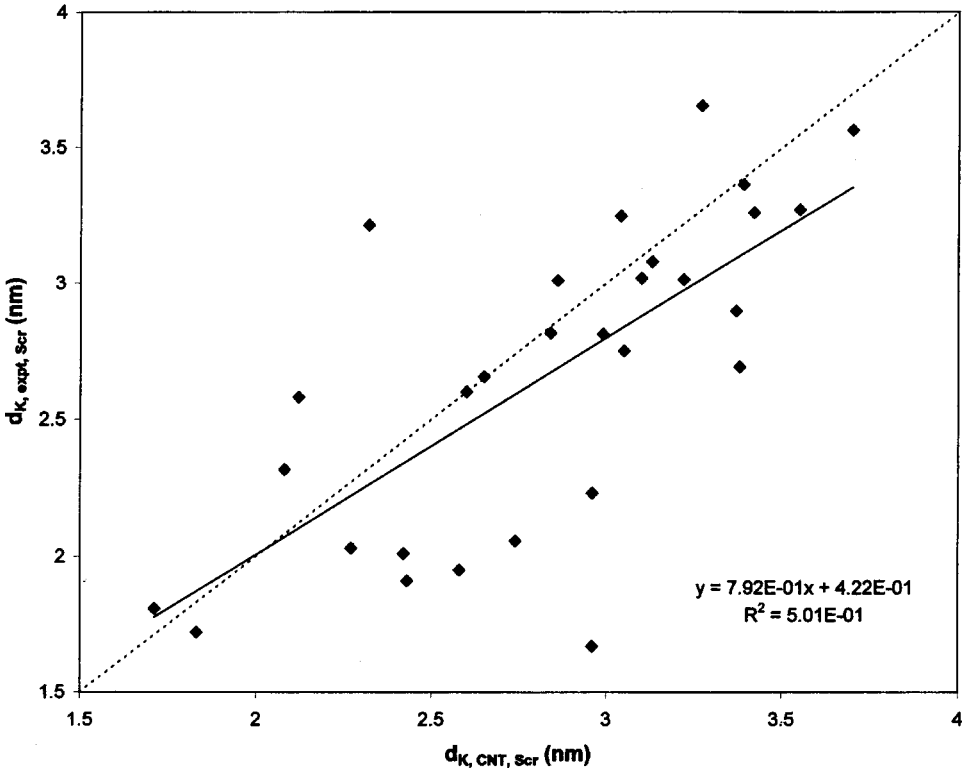

FIG. 8. Plot of $d_{K,\ expt,\ Scr}$ (Kelvin diameter calculated from experimentally determined critical supersaturation) versus $d_{K,CNT,Scr}$ (Kelvin diameter calculated from CNT). Freon 11 was excluded from the plot. There is a moderate correlation between experiment and theory. The correlation becomes somewhat higher if the carboxylic acids are also excluded. The dotted line represents the ideal one-to-one relationship.

TABLE 3. Kelvin diameter (d_K) at 300 K using experimentally determined or CNT-predicted critical supersaturation. The left hand side of the table is sorted according to d_K based on experimental supersaturation while the right hand side is sorted according to d_K predicted from CNT. Note that the number caption is different from those used in the figures

Sorted according to $d_{K,expt}$			Sorted according to $d_{K,CNT}$		
Number	Fluid	$d_{K,expt}$	$d_{K,expt}$ number	Fluid	$d_{K,CNT}$
1	acetic acid	1.67	3	glycerol	1.71
2	water	1.72	2	water	1.83
3	glycerol	1.81	10	ethylene glycol	2.08
4	benzonitrile	1.91	11	trimethylene glycol	2.12
5	nitromethane	1.95[a]	7	nitrobenzene	2.27
6	decanoic acid	2.01	23	propylene glycol	2.32
7	nitrobenzene	2.03	6	decanoic acid	2.42
8	myristic acid	2.06	4	benzonitrile	2.43
9	acetonitrile	2.23	5	nitromethane	2.58
10	ethylene glycol	2.32	12	1,1,2,2-tetrachloroethane	2.60
11	trimethylene glycol	2.58	13	heptanoic acid	2.65
12	1,1,2,2-tetrachloroethane	2.60	8	myristic acid	2.74
13	heptanoic acid	2.66	17	*n*-butylbenzene	2.84
14	methanol	2.69	19	*o*-xylene	2.86
15	chloroform	2.75	1	acetic acid	2.96
16	toluene	2.81	9	acetonitrile	2.96
17	*n*-butylbenzene	2.81	16	toluene	2.99
18	ethanol	2.90	24	*n*-pentanol	3.04
19	*o*-xylene	3.01	15	chloroform	3.05
20	*n*-propanol	3.01	21	carbon tetrachloride	3.10
21	carbon tetrachloride	3.02	22	*n*-butanol	3.13
22	*n*-butanol	3.08	20	*n*-propanol	3.22
23	propylene glycol	3.21	29	*n*-nonane	3.27
24	*n*-pentanol	3.25	18	ethanol	3.37
25	2-propanol	3.26	14	methanol	3.38
26	heptane	3.27	27	octane	3.39
27	octane	3.36	25	2-propanol	3.42
28	hexane	3.56	26	heptane	3.55
29	*n*-nonane	3.65	28	hexane	3.70

[a]The extrapolated value for nitromethane is somewhat questionable due to nonlinear variation of the Kelvin diameter for this fluid.

rectly predicts water and glycerol as having the smallest Kelvin diameter.

However, although it does predict the general trend for the rest of the data, the internal order between the Kelvin diameters for the fluids is not correctly predicted in several cases. For example, for the *n*-alcohols, the Kelvin diameter, in conflict with the theoretical predictions, actually generally increases with increasing surface tension. It should, however, be noted that the *n*-alcohols have relatively similar surface tensions, giving room for experimental errors to play a larger role, but the trend still is clearly opposite to that predicted from theory.

In spite of the noted exceptions, it can generally be said that the fluid with the highest surface tension will have the lowest Kelvin diameter. The trend is somewhat more pronounced if the molecular weight is also taken into account: a fluid with high surface tension in combination with low molecular weight generally has a lower Kelvin diameter. Given the generally very high surface tension of liquid metals, this qualitative predictor would imply that metal vapors should be able to activate the growth of exceedingly small clusters. A thorough discussion of the issue falls beyond the scope of this work, but sufficient information for its clarification can be found in the study by Fisk *et al.* (1998). Although available information on the anomalously low critical supersaturation of mercury would have led to pessimism, more recent studies on cesium nucleation at 359 K reveal a critical cluster size (based on the Kelvin diameter) of 12 atoms! If a cesium vapor CNC were viable or practical, it would be able to detect uncharged particles of subnanometer dimensions.

4.3. Correlation of Kelvin Diameter with the Dielectric Constant

Glycerol and water have the lowest calculated Kelvin diameters and, in addition to having particularly high surface tensions, have some other similarities, one of these being high polarity. The relative dielectric constant (ε) is the most commonly used measure of solvent polarity [e.g., Brown (1995)]. A solvent is arbitrarily considered polar if it has a dielectric constant of 20 or greater, and is nonpolar if the dielectric constant is less than that. The dielectric constants for glycerol and water are 42.5 [Lide (1995)] and 78.5 [Lide (1992)], respectively at 298 K, while those for very nonpolar substances such as *n*-hexane and *n*-nonane are about 1.9–2.0. It was found that for the compound class of glycols and the closely related glycerol, the Kelvin diameter generally de-

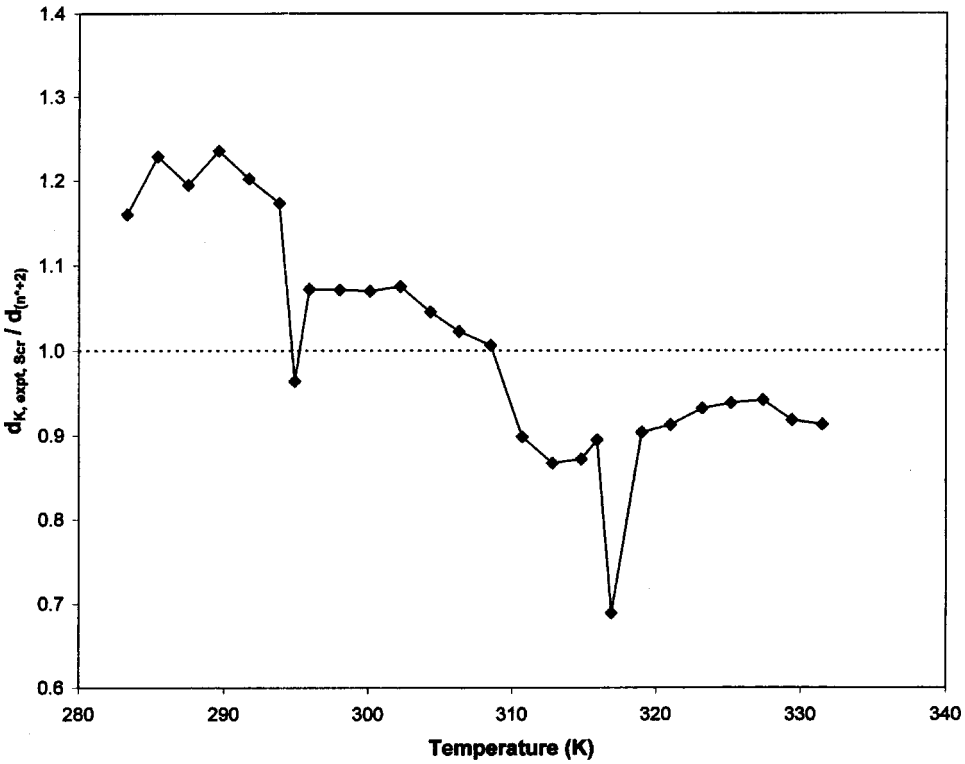

FIG. 9. Plot of Kelvin diameter divided by the diameter calculated from the number of molecules in the critical embryo, versus temperature for glycerol. The ''jumps'' at about 295 and 317 K are due to phase transitions in the critical embryo [see Anisimov *et al.* (1998)]. The dotted line represents a ratio of 1. The agreement between the Kelvin diameter and the diameter calculated from the number of molecules in the critical embryo is reasonable.

creased as ε increased (see Fig. 14). This spurred a deeper investigation into the relationship between dielectric constant and Kelvin diameter.

Among the 30 investigated fluids, a few compound classes are represented, such as *n*-alcohols, *n*-alkanes, arenes, carboxylic acids, chlorinated hydrocarbons, and glycols. Of these compound classes, five are represented by more than two closely related fluids within the class, namely *n*-alcohols, *n*-alkanes, carboxylic acids, chlorinated hydrocarbons, and glycols. Of these, the data for acetic acid are questionable due to association, and ε for myristic, decanoic and heptanoic acids could not be found in the literature. In addition, as mentioned previously, the data for the carboxylic acids are among the least reliable [see Agarwal and Heist (1980)] and fairly long extrapolations had to be done in order to get a value for the Kelvin diameter at 300 K. Thus, the carboxylic acids class was excluded from continued investigation.

Dielectric constant data were obtained from Lide (1992) and from Lide (1995). These data are most often given as values measured at 293 or 298 K. Kelvin diameters at 300 K were extracted from the data used to generate Fig. 6. The temperature of 300 K was chosen because values for the Kelvin diameter could be obtained with little or no extrapolation for most of the fluids at this temperature (short linear extrapolations were done to obtain the data for carbon tetrachloride, *n*-heptane, *n*-octane, propylene glycol, and trimethylene glycol). Longer extrapolations were needed for chloroform and hexane.

Figure 15 shows the Kelvin diameter at 300 K versus the 10-logarithm of the relative dielectric constant. Glycerol is included with the glycols in this plot. The dielectric constant is generally 1.9–2.0 for the *n*-alkanes, and any trend in those data may be masked by experimental uncertainties. However, within each of the three other compound classes (*n*-alcohols, chlorinated hydrocarbons, and glycols), there is a trend toward lower Kelvin diameter as the dielectric constant increases. It is interesting to note that the trend for the *n*-alcohols is correctly correlated with the dielectric constant, which was not the case when correlated with the surface tension.

It should also be mentioned that there are some substituted arenes among the 30 investigated fluids (*n*-butylbenzene, *o*-xylene, toluene, nitrobenzene, and benzonitrile). These fluids were not included in Fig. 15, because they were considered not very closely related (except for *o*-xylene and toluene) other than by the benzene ring. However, the general trend among these fluids is that the low-dielectric constant fluids (*n*-butylbenzene, *o*-xylene, and toluene) have higher Kelvin diameters while the higher-dielectric constant fluids (nitrobenzene and benzonitrile) have lower Kelvin diameters.

The correlation between the Kelvin diameter and the dielectric constant can partly be explained by a relationship between dielectric constant and surface tension, found by Papazian (1971) [see also Holmes (1973) and Papazian (1986)]. The relationship was linear for σ versus $(\varepsilon-1)/(2\varepsilon+1)$ or simply for σ versus ε [Holmes (1973)]. However, the relationship held only for nonpolar liquids with zero dipole moment. No correlation was found between σ and ε for polar liquids. However, when Papazian eliminated the dipolar contribution to the dielectric constant by using the Maxwell relation [e.g., see Smith (1955)] $\varepsilon=n^2$, where n

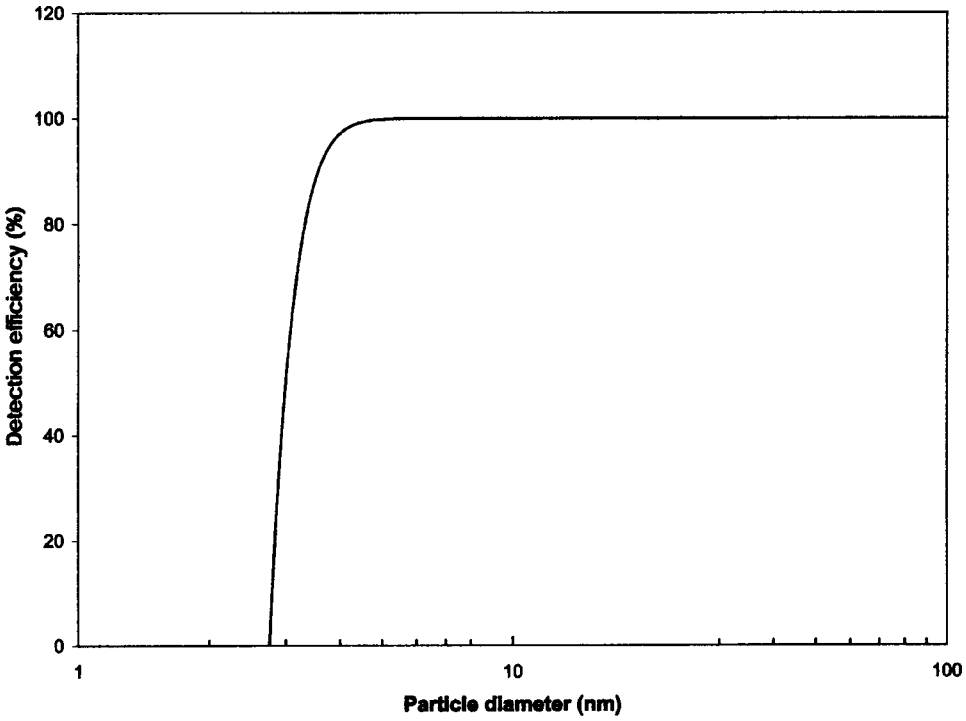

FIG. 10. Detection efficiency curve for the TSI UCPC 3025A [Kesten *et al.* (1991)].

is refractive index, a fairly good correlation was obtained between σ and n^2 when strongly hydrogen-bonding liquids were excluded.

However, using the present data, it can be seen that there is in fact a linear positive correlation between dielectric constant and surface tension for the fluids within the classes of glycols and *n*-alkanes, while the correlation is nonlinear but strongly positive for the presently considered chlorinated hydrocarbons. Papazian did not find these correlations, because he did not divide the data into separate classes. In contrast, the correlation for the *n*-alcohols is linear but negative. Recalling that the correlation between the Kelvin diameter and the surface tension was, in contrast to the CNT, positive for *n*-alcohols, a combination of these two correlations together leads to the negative correlation between Kelvin diameter and dielectric constant for the case of *n*-alcohols.

When looking at other classes of fluids, including some of those for which no experimental nucleation data are presently available, it was found that a correlation between surface tension and dielectric constant exists for various classes of fluids (Fig. 16). The values for surface tension were mostly given by the data source [Lide (1995)] at 298 or 293 K, and the dielectric constant was mostly given at 293 K but sometimes at other temperatures.

As seen in the figure, the correlation is sometimes positive and sometimes negative. However, it seems to be fairly linear in most cases if the class members are chosen narrowly enough. So it was found that, like the normal monohydroxylated alcohols (1-substituted), the 2-substituted monohydroxylated alcohols (2-propanol, 2-butanol, 2-pentanol and 2-octanol) exhibit a negative linear correlation. Similar negative linear correlations were also found for 1-chloroalkanes (chloromethane, chloroethane, 1-chloropropane, 1-chlorobutane, 1-chloropentane and 1-chlorooctane) and nitrilalkanes (ethane, propane, butane, pentane and octanenitrile). However, in the case of nitrilalkanes, ethanenitrile (acetonitrile, the most polar) deviates upward from the line, while the others adhere very well to the line. The same is true for the *n*-alcohols, where methanol (most polar) deviates from the line towards higher surface tensions. Long-chain carboxylic acids (5–9 carbons) also have an almost linear negative correlation.

Classes having positive linear correlations include the short-chain carboxylic acids (1–4 carbons), glycols with hydroxyl groups at both ends of the chain and the nitroalkanes (nitromethane, nitroethane, and 1-nitropropane). The *n*-alkanes also have a positive correlation, although the line is almost parallel to the σ-axis. Looking at Fig. 16, it seems like the lines ''fan'' out so that the correlation becomes more positive (or less negative) the higher the general polarity (dielectric constant) of the class is.

Since experimental critical supersaturation data are not available for most of the other fluid classes for which the correlation between surface tension and dielectric constant is negative, it is not possible to say whether these fluids, like the 1-alcohols, also exhibit decreasing Kelvin diameters with increasing dielectric constant. At this point, the limited amount of data available clearly indicate a relationship between the Kelvin diameter and the dielectric constant of the fluid, at least within the class of the fluid. It should also be pointed out that water, having the lowest Kelvin diameter of the 30 investigated fluids, also has a particularly high relative dielectric constant.

Thus, assuming that the correlation between Kelvin diameter and dielectric constant extends to the fluids for which nucleation data are presently unavailable, this discovery pro-

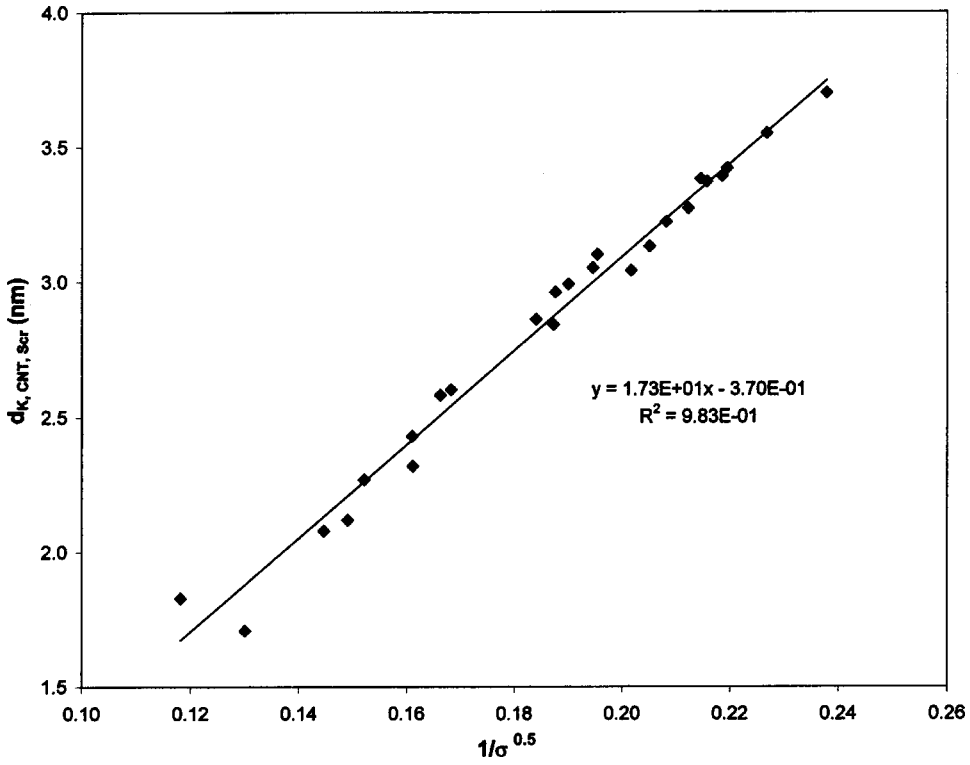

FIG. 11. The CNT-estimated Kelvin diameter at 300 K plotted versus the square root of the reciprocal surface tension. The data points adhere fairly well to a straight line. The carboxylic acids and Freon 11 are excluded in this plot.

vides a simple and fast method for finding superior condensing fluids, since data for dielectric constant are much more widely available than are critical supersaturation data. For example, if one knew the Kelvin diameter for one fluid in a particular compound class, the efficacy for growing small particles of any other fluid within that class, relative to that of the known fluid, could be estimated based on the dielectric constant. Thus, within a class of fluids, the fluid with the highest dielectric constant would provide the lowest Kelvin diameter and thereby provide the possibility to grow and detect smaller particles. These conclusions are all based on empirical observations of literature data. However, it would

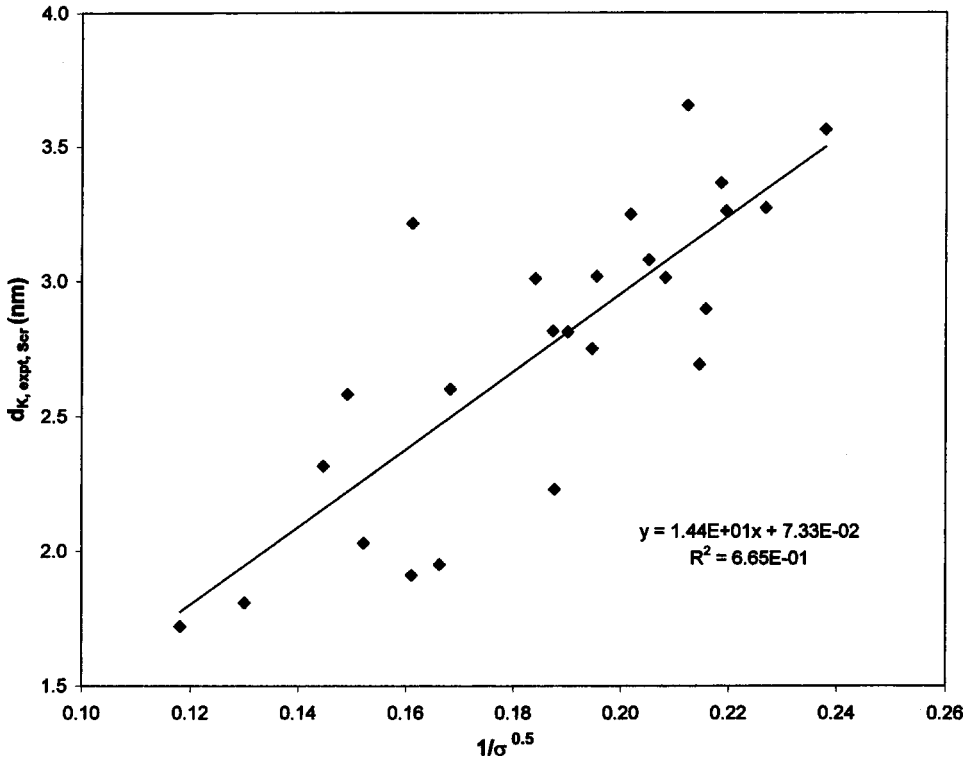

FIG. 12. The Kelvin diameter calculated based on experimental critical supersaturation at 300 K plotted versus the square root of the reciprocal surface tension. The squared correlation coefficient of about 0.67 for a linear regression suggests a fairly strong relation between Kelvin diameter and the square root of the reciprocal surface tension. The trend for fluids with higher surface tensions having lower Kelvin diameters and vice versa is relatively clear. The carboxylic acids and Freon 11 are excluded in this plot.

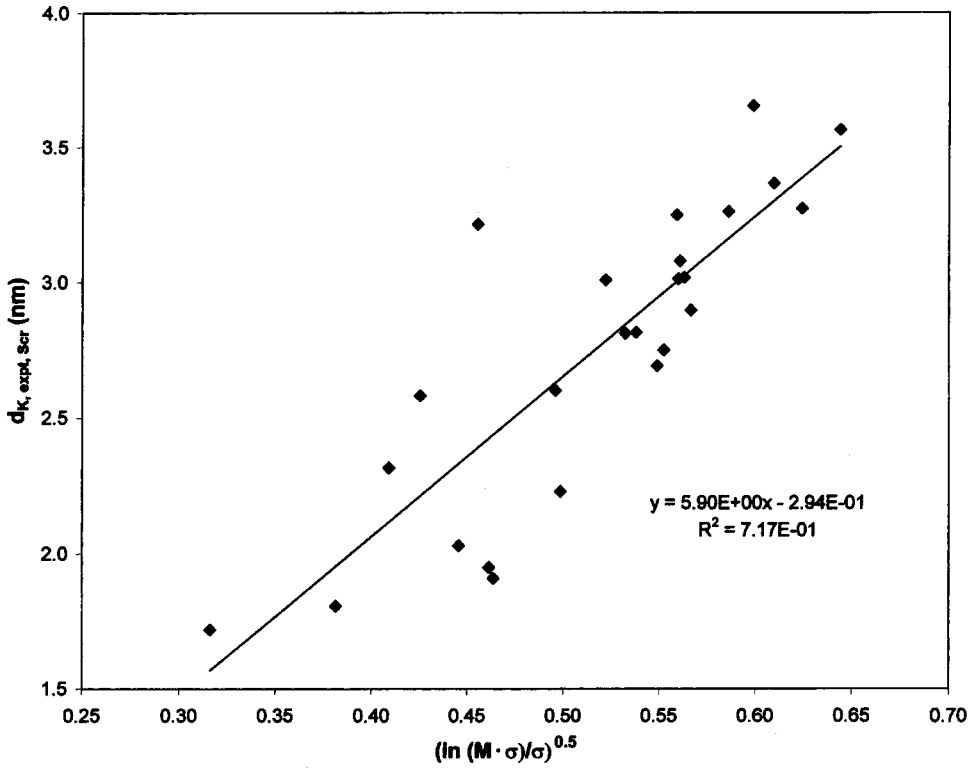

FIG. 13. The Kelvin diameter calculated based on experimental critical supersaturation at 300 K plotted versus the square root of $\ln(M \cdot \sigma)/\sigma$. The squared correlation coefficient is about 0.72 for a linear regression, which is slightly higher than the correlation obtained when plotting versus the square root of the reciprocal surface tension. The trend for fluids with higher surface tensions and lower molecular weights having lower Kelvin diameters and vice versa is relatively clear. The carboxylic acids and Freon 11 are excluded in this plot.

be desirable to have some kind of theoretical understanding of the relationship between the dielectric constant and the Kelvin diameter.

A few papers aimed at investigating nucleation of polar and hydrogen bonding molecules have been published, mostly from the group of M. Samy El-Shall [e.g., Wright *et al.* (1993); Wright and El-Shall (1993); Kane and El-Shall (1996)]. In their 1993 work, Wright and El-Shall suggested two possible models for explaining the nucleation behavior of polar molecules. The first model is based upon work by

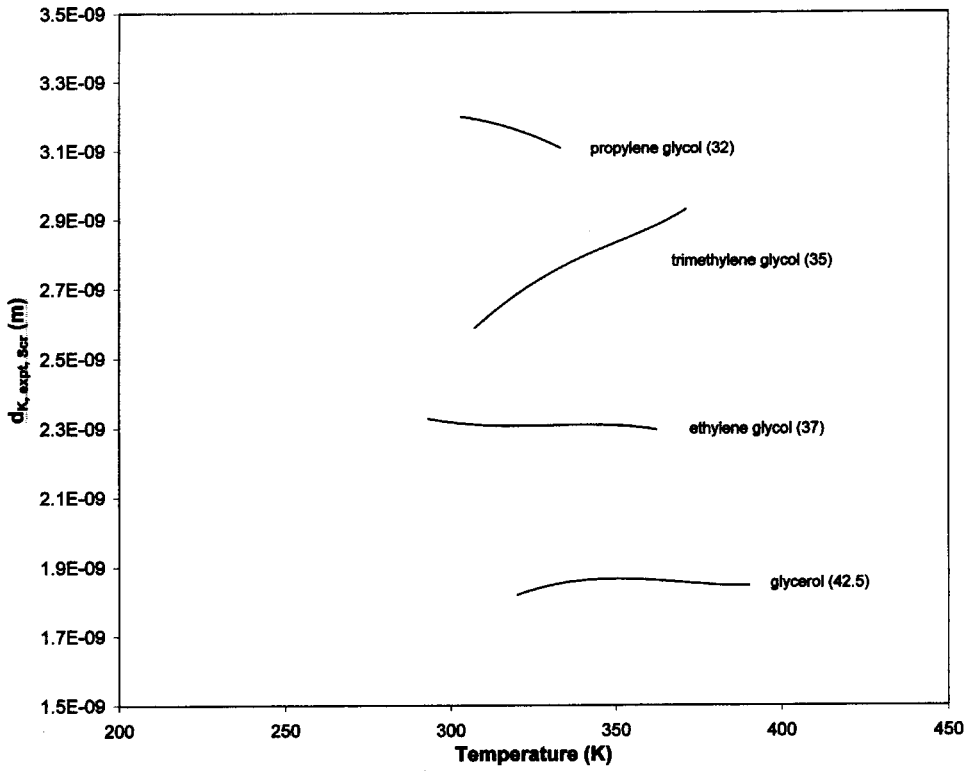

FIG. 14. Kelvin diameters for the glycols propylene glycol (1,2-propanediol), trimethylene glycol (1,3-propanediol), diethylene glycol (1,2-ethanediol), and glycerol (1,2,3-propanetriol). The dielectric constant for each fluid is given in parenthesis.

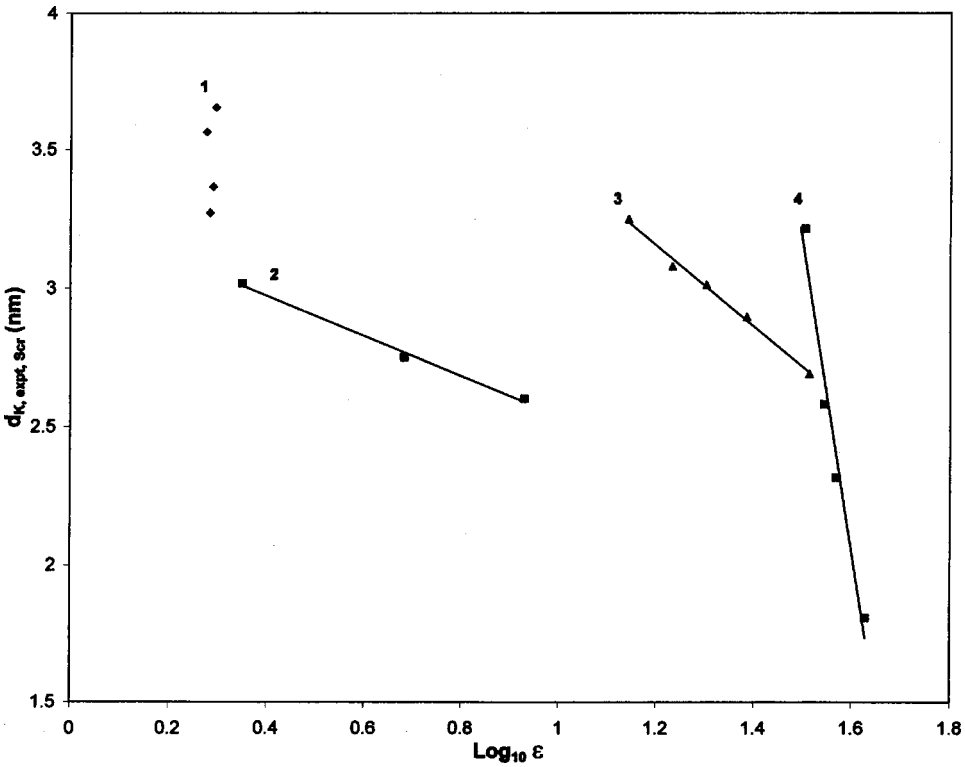

FIG. 15. Kelvin diameter at 300 K versus the 10-logarithm of the dielectric constant for (1) *n*-alkanes, (2) chlorinated hydrocarbons, (3) *n*-alcohols, and (4) glycols (including glycerol).

Abraham [e.g., Abraham (1969)], in which the surface tension of an embryonic droplet is suggested to increase with decreasing radius of the droplet due to dipole–dipole interactions that cause the molecules in the droplet to be highly oriented at the surface of the droplet. See Wright and El-Shall (1993) for a more in-depth discussion. This amounts to a curvature-dependent surface tension specifically for polar compounds. This would generally cause an increase in the critical supersaturation for polar fluids, and therefore also smaller critical cluster sizes. However, the acceptable agree-

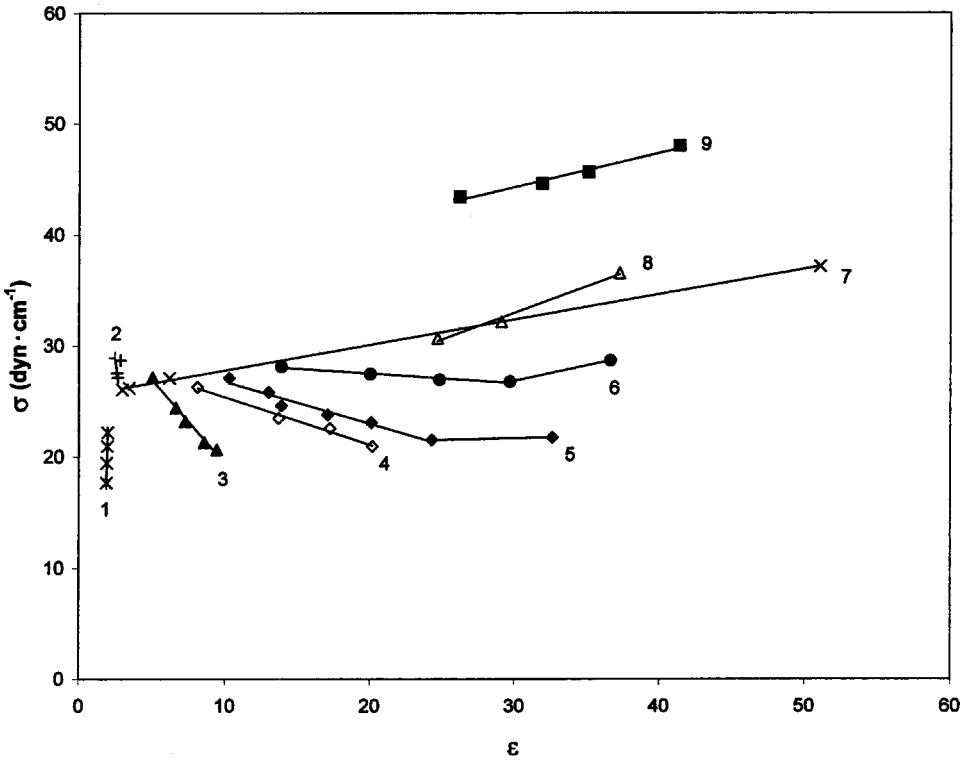

FIG. 16. The correlation between surface tension and dielectric constant for several classes of fluids. The classes are (1) *n*-alkanes, (2) long-chain carboxylic acids, (3) 1-chloroalkanes, (4) 2-alcohols, (5) 1-alcohols, (6) nitrilalkanes, (7) short-chain carboxylic acids, (8) 1-nitroalkanes and (9) glycols (with the hydroxyl groups at each end). The correlation seems to tend to be more positive (or less negative) the higher the general polarity of the class is. In addition, the most polar substances in the classes of 1-alcohols and nitrilalkanes (methanol and acetonitrile) deviate from the line toward higher surface tensions.

ment between the Kelvin diameter and the diameter calculated from the number of molecules in the critical embryo for glycerol does not support a significant change of surface tension from the bulk values.

The other suggested model for nucleation behavior of polar molecules is based on a change from assuming that the embryos are spherical in shape. Instead, it was thought that polar molecules might orient themselves in the embryo in such a way that the embryo will take on a prolate spheroid shape. This was discussed and found feasible, at least for acetonitrile [Wright and El-Shall (1993)]. The change in shape from purely spherical would cause an increase in surface free energy (surface tension) and therefore a higher critical supersaturation and possibly smaller critical embryo sizes. It is hard to verify this model without making significant calculations and assumptions about the orientation of molecules in the various investigated fluids. Suffice it to say that this model might have some validity to it, and it may be interesting to investigate this further in a separate work. However, it should also be pointed out that not all of the polar molecules have especially high critical supersaturation (Fig. 3).

In conclusion, these models do support a different nucleation behavior for polar molecules, although it is hard to verify them quantitatively from the data. More systematic nucleation research in this area would be needed.

5. Conclusions

In this paper, Kelvin diameters at critical supersaturation were calculated from experimental data for 30 fluids. Based on these results, it can be concluded that some substances may be more suitable than others for use in techniques based on vapor condensation, such as condensation particle counting and condensation nucleation light scattering detection, when the goal is to detect as small particles as possible. Two fluids of particular interest are glycerol and water, since their Kelvin diameters were found to be particularly low compared to the other fluids investigated. However, some researches have suggested that the Kelvin equation might not be valid for water droplets of very small diameters. On the other hand, fair agreement was found between the Kelvin diameter for glycerol and the diameter calculated by an independent method (the Nucleation theorem) based on the number of molecules in the glycerol critical embryo.

From the CNT, it was found that the surface tension is generally the most important factor in determining the Kelvin diameter. The Kelvin diameter is generally lower when the surface tension is higher. This provides helpful guidance in choosing the best fluids for purposes of growing as small particles as possible. However, the agreement between experimentally determined Kelvin diameters and the Kelvin diameters predicted by the CNT was only moderate and it was found that the trend based on surface tension is not true for all cases. In particular, the trend was found to be the opposite for the *n*-alcohols.

It was also found that the Kelvin diameter correlated with the dielectric constant of a fluid in such a way that the Kelvin diameter was lower for fluids with higher dielectric constant. This was found to be true for fluids within their particular chemical class, including the *n*-alcohols. It is unknown whether the relationship extends to fluids for which nucleation data are presently unavailable. The relationship was partly explained by a relationship between surface tension and dielectric constant for a fluid.

A method for choosing the best condensing fluid, from the standpoint of growing as small particles as possible, was devised based on the correlation between Kelvin diameter and dielectric constant. According to this method, the fluid having the highest dielectric constant, within its chemical class, will have the lowest Kelvin diameter and will thus facilitate the growth and detection of the smallest particles.

The results presented in this paper provide guidance for the rational selection of alternate substances to investigate for the reduction of the threshold sizes of condensation-based detection devices, leading to higher sensitivities for techniques such as CNLSD, i.e.:

(1) The fluid with the highest surface tension will have the lowest Kelvin diameter. The trend is somewhat more pronounced if the molecular weight is also taken into account: a fluid with high surface tension in combination with low molecular weight generally has a low Kelvin diameter.
(2) Within a class of fluids, the fluid with the highest dielectric constant will generally provide the lowest Kelvin diameter and thereby provide the possibility to grow and detect smaller particles.

6. Acknowledgments

The work done at Clarkson University was supported by the National Science Foundation under Grant No. CTS 9976615. The work done at SIUC was supported by the National Science Foundation under Grant No. CHE-9311427, and by Evotec Biosystems, GMBh.

7. References

Abraham, F. F., J. Chem. Phys. **50**, 3977 (1996).
Agarwal, G. and R. H. Heist, J. Chem. Phys. **73**, 902 (1980).
Agarwal, J. K. and G. J. Sem, J. Aerosol Sci. **11**, 343 (1980).
Allen, L. B. and J. A. Koropchak, Anal. Chem. **65**, 841 (1993).
Alofs D. J., C. K. Lutrus, D. E. Hagen, G. J. Sem, and J. L. Blesener, Aerosol Sci. Tech. **23**, 239 (1995).
Anisimov, M. P., V. G. Costrovskiy, and M. S. Schtein, Kolloid. Zh. (Russian) **40**, 317 (1978).
Anisimov, M. P., P. K., Hopke, S. D. Shandakov, and I. I. Shvets, J. Chem. Phys. **113**, 1971 (2000).
Anisimov, M. P., J. A. Koropchak, A. G. Nasibulin, and L. V. Timoshina, J. Chem. Phys. **109**, 10004 (1998).
Anisimov, M. P., A. G. Nasibulin, S. D. Shandakov, and I. N. Shaimordanov, Colloid J. **63**, 131 (2001). [Translated from Kolloidnyi Zhurnal **63**, 149 (2001)].
Becker, R. and W. Döring, Annalen Physik **24**, 719 (1935).
Brown, W. H., *Organic Chemistry* (Harcourt Brace & Co., Orlando, FL, 1995).

Chen, D.-R., D. Y. H. Pui, and S. L. Kaufman, J. Aerosol Sci. **26**, 963 (1995).
Costello, J. M. and S. T. Bowden, Rec. Trav. Chim. **77**, 803 (1958).
Dillmann, A. and G. E. A. Meier, J. Chem. Phys. **94**, 3872 (1991).
Ekbom, L., *Tabeller och formler, tredje upplagan* (Almqvist & Wiksell Förlag AB, Stockholm, 1991).
Everett, D. H. and J. M. Haynes, Colloid Sci. **1**, 123 (1973).
Felder, R. M. and R. W. Rousseau, *Elementary Principles of Chemical Processes*, 2nd ed. (Wiley, New York, 1986).
Fenelonov, V. B., G. G. Kodenyov, and V. G. Kostrovsky, J. Phys. Chem. B **105**, 1050 (2001).
Fisher, L. R., Adv. Colloid Interface Sci. **16**, 117 (1982).
Fisher, L. R. and J. N. Israelachvili, Colloids Surfaces **3**, 303 (1981).
Fisk J. A., M. M. Rudek, J. L. Katz, D. Beiersdof, and H. Uchtmann Atmospheric Research **46**, 211 (1998).
Gamero-Castaño, M. and J. Fernández de la Mora, J. Aerosol Sci. **31**, 757 (2000).
Hales, J. L. and R. Townsend, J. Chem. Thermodyn. **4**, 763 (1972).
Heide, R., Luft Kältetech. **9**, 125 (1973).
Heist, R. H., J. Phys. Chem. **99**, 16792 (1995).
Heist, R. H., K. M. Colling, and C. S. Dupuis, J. Chem. Phys. **65**, 5147 (1976).
Heist, R. H. and H. He, J. Phys. Chem. Ref. Data **23**, 781 (1994).
Helsper, C. and R. Nießner, J. Aerosol Sci. **16**, 457 (1985).
Holmes, C. F., J. Am. Chem. Soc. **95**, 1014 (1973).
Hunten, K. W. and O. Maass, J. Am. Chem. Soc. **51**, 153 (1929).
Hunter, R. J., *Foundations of Colloid Science*, Vol. I (Clarendon, Oxford, 1987).
IAPWS Industrial Formulation 1997 for the Thermodynamic Properties of Water and Steam (The International Association for the Properties of Water and Steam, Erlangen, Germany, 1997).
The International Critical Tables, Vol. III and IV (McGraw–Hill, New York, 1928).
Jasper, J. J., J. Phys. Chem. Ref. Data **1**, 841 (1972).
Jasper, J. J. and E. V. Kring, J. Phys. Chem. **59**, 1019 (1955).
Kane, D. and M. S. El-Shall, J. Chem. Phys. **105**, 7617 (1996).
Katz, J. L., J. Chem. Phys. **52**, 4733 (1970).
Katz, J. L., P. Mirabel, C. J. Scoppa, and T. L. Virkler, J. Chem. Phys. **65**, 382 (1976).
Katz, J. L., C. J. Scoppa, N. G. Kumar, and P. Mirabel, J. Chem. Phys. **62**, 448 (1975).
Kesten, J., A. Reineking, and J. Porstendörfer, Aerosol Sci. Tech. **15**, 107 (1991).
Koropchak, J. A., M. P. Anisimov, and L.-E. Magnusson, U.S. Patent Pending (2000).
Koropchak, J. A., L.-E. Magnusson, M. Heybroek, S. Sadain, X. Yang, and M. P. Anisimov, Fundamental Aspects of Aerosol-Based Light-Scattering Detectors for Separations, in *Advances in Chromatography*, edited by P. R. Brown and E. Grushka (Marcel Dekker, New York, 2000), 275–314.
Koropchak, J. A., S. Sadain, X. Yang, L.-E. Magnusson, M. Heybroek, M. P. Anisimov, and S. L. Kaufmann, Anal. Chem. **71**, 386A (1999).
Lide, D. R., editor, *CRC Handbook of Chemistry and Physics*, 72nd ed. (Chemical Rubber Corp., Boca Raton, FL, 1992).
Lide, D. R., editor, *CRC Handbook of Thermophysical and Thermochemical Data* (Chemical Rubber Corp., Boca Raton, FL, 1994).
Lide, D. R., *Handbook of Organic Solvents* (Chemical Rubber Corp., Boca Raton, FL, 1995).
Liu, B. Y. H., D. Y. H. Pui, R. L. McKenzie, J. K. Agarwal, F. G. Pohl, O. Preining, G. Reischl, W. Szymanski, and P. E. Wagner, Aerosol Sci. Tech. **3**, 107 (1984).
Magnusson, L.-E. Ph.D. Dissertation, Southern Illinois University at Carbondale, 2002.
Magnusson, L., M. P. Anisimov, and J. A. Koropchak, The 25th Annual Conference of the Federation of Analytical Chemistry and Spectroscopic Societies, Austin, TX, 1998.
Mavliev, R., P. K. Hopke, H.-C. Wang, and D.-W. Lee, Aerosol Sci. Tech. **35**, 586 (2001).
McDermott, W. T., R. C. Ockovic, and M. R. Stolzenburg, Aerosol Sci. Tech. **14**, 278 (1991).
McDonald, J. E., Am. J. Phys. **30**, 870 (1962).
McMurry, P. H., Aerosol Sci. Tech. **33**, 297 (2000).
Melrose, J. C., Am. Inst. Chem. Engrs. J. **12**, 986 (1966).
Melrose, J. C., J. Colloid Interface Sci. **38**, 312 (1972).
Melrose, J. C., Langmuir **5**, 290 (1989).
Papazian, H. A., J. Am. Chem. Soc. **93**, 5634 (1971).
Papazian, H. A., J. Am. Chem. Soc. **108**, 3239 (1986).
Parsons, C. and R. Mavliev, Aerosol Sci. Tech. **34**, 309 (2001).
Porstendörfer, J., H. G. Scheibel, F. G. Pohl, O. Preining, G. Reischl, and P. E. Wagner, Aerosol Sci. Tech. **4**, 65 (1985).
Rebours, A. B., D. Boulaud, and A. Renoux, J. Aerosol Sci. **27**, 1227 (1996).
Rein ten Wolde, P., D. W. Oxtoby, and D. Frenkel, J. Chem. Phys. **111**, 4762 (1999).
Rudek, M. M., J. A. Fisk, V. M. Chakarov, and J. L. Katz, J. Chem. Phys. **105**, 4707 (1996).
Selected Values of Properties of Hydrocarbons and Related Compounds (American Petroleum Institute, College Station, TX, 1965), now located at NIST, Boulder, CO.
Smith, J. W., *Electric Dipole Moments* (Butterworths, London, 1955).
Stolzenburg, M. R. and P. H. McMurry, Aerosol Sci. Tech. **14**, 48 (1991).
Strey, R. and T. Schmeling, Ber. Bunsenges. Phys. Chem. **87**, 324 (1983).
Szostek, B., J. Zajac, and J. A. Koropchak, Anal. Chem. **69**, 2955 (1997).
Timmermans, J., *Physico-Chemical Constants of Pure Organic Compounds* (Elsevier, New York, 1950), pp. 380–382.
Vargaftik, N. B., *Tables on the Thermophysical Properties of Liquids and Gases in Normal and Dissociated States*, 2nd ed. (Wiley, New York, 1975), pp. 422–423.
Vargaftik, N. B., B. N. Volkov, and L. D. Voljak, J. Phys. Chem. Ref. Data **12**, 817 (1983).
Wiedensohler, A., D. Orsini, D. S. Covert, D. Coffmann, W. Cantrell, M. Havlicek, F. J. Brechtel, L. M. Russel, R. J. Weber, J. Gras, J. G. Hudson, and M. Litchy, Aerosol Sci. Tech. **27**, 224 (1997).
Wilson, C. T. R., *On the Cloud Method of Making Visible Ions and the Tracks of Ionizing Particles*, in *Nobel Lectures Physics* (Elsevier, New York, 1927).
Wright, D., R. Caldwell, C. Moxley, and M. S. El-Shall, J. Chem. Phys. **98**, 3356 (1993).
Wright, D. and M. S. El-Shall, J. Chem. Phys. **98**, 3369 (1993).
Yaws, C., *Handbook of Vapor Pressure* (Gulf Publishing Co., Houston, TX, 1994).